DAHLGREN DIVISION
NAVAL SURFACE WARFARE CENTER
Dahlgren, Virginia 22448-5100

NSWCDD/TR-00/67

IMPROVED POWER-ON, BASE DRAG METHODOLOGY FOR THE AEROPREDICTION CODE

BY FRANK G. MOORE
AEROPREDICTION, INC.

THOMAS C. HYMER
NSWCDD

WEAPONS SYSTEMS DEPARTMENT

MAY 2001

REPORT DOCUMENTATION PAGE

Form Approved
OMB No. 0704-0188

1. AGENCY USE ONLY (Leave blank)	2. REPORT DATE	3. REPORT TYPE AND DATES COVERED
	May 2001	Final

4. TITLE AND SUBTITLE

Improved Power-on, Base Drag Methodology for the Aeroprediction Code

5. FUNDING NUMBERS

6. AUTHOR(s)

Frank G. Moore, Thomas C. Hymer

7. PERFORMING ORGANIZATION NAME(S) AND ADDRESS(ES)

Commander
Naval Surface Warfare Center
Dahlgren Division (Code G23)
17320 Dahlgren Road
Dahlgren, VA 22448-5100

8. PERFORMING ORGANIZATION REPORT NUMBER

NSWCDD/TR-00/067

9. SPONSORING/MONITORING AGENCY NAME(S) AND ADDRESS(ES)

10. SPONSORING/MONITORING AGENCY REPORT NUMBER

11. SUPPLEMENTARY NOTES

12a. DISTRIBUTION/AVAILABILITY STATEMENT

Approved for public release; distribution is unlimited.

12b. DISTRIBUTION CODE

13. ABSTRACT (Maximum 200 words)

Improved methods for base pressure prediction under base bleed and rocket motor-on conditions have been developed. The base bleed method makes several refinements to the method developed by Danberg at the Army Research Laboratory in Aberdeen, Maryland. The improved rocket motor-on, base pressure prediction improves upon the method developed at the Army Missile Command in Huntsville, Alabama by Brazzel and some of his colleagues. The major refinement to the base bleed method of Danberg was to estimate the power-off value of base pressure empirically based on an extensive data base, as opposed to using computational fluid dynamics codes to predict this term. The major modifications to the power-on base pressure prediction method of Brazzel was to extend its range of applicability to high values of thrust coefficient, to Mach numbers less than 1.5, and to different afterbody shapes.

In comparing the improved methods for power-on base drag prediction to experiment, it was seen that both methods gave reasonable agreement to most experimental data bases. However, more validation is needed, particularly for the combined effects of angle of attack, fins, and power-on conditions.

14. SUBJECT TERMS

aerodynamics, Aeroprediction Code, power-on base drag, base bleed

15. NUMBER OF PAGES

76

16. PRICE CODE

17. SECURITY CLASSIFICATION OF REPORTS	18. SECURITY CLASSIFICATION OF THIS PAGE	19. SECURITY CLASSIFICATION OF ABSTRACT	20. LIMITATION OF ABSTRACT
UNCLASSIFIED	UNCLASSIFIED	UNCLASSIFIED	UL

FOREWORD

The 1998 version of the aeroprediction code (AP98) used a semiempirical method to compute the effects of a rocket motor on the base drag. This method required inputs from users that in many cases were not known. As a result, many users of the AP98 would choose not to use the power-on base drag prediction capability of the AP98. Also, no alternative exists in the AP98 to predict base bleed effects on base drag for projectile configurations. The work described in this report attempts to minimize these shortcomings of the AP98. These shortcomings are eliminated by giving the user several alternatives for computing power on base drag for rockets (some of which require no details of the rocket motor), and by incorporating a method to predict the effect on base pressure of base bleed.

The work described in this report was supported by the Office of Naval Research through the Surface Weapons Systems Technology Program managed at the Naval Surface Warfare Center, Dahlgren Division (NSWCDD) by Mr. Robin Staton. Tasking from this program was provided by Mr. Roger Horman and Mr. John Fraysse. The authors express appreciation for support received in this work.

Approved by:

DANNY BRUNSON, Head
Weapons Systems Department

CONTENTS

Section		Page
1.0	INTRODUCTION	1
2.0	ANALYSIS	2
	2.1 POWER-ON BASE DRAG FOR $M_j \geq 1.0$	2
	2.2 BASE BLEED	13
	2.3 MODIFIED BASE DRAG PREDICTION MODEL	17
3.0	RESULTS AND DISCUSSION	27
	3.1 BASE BLEED	27
	3.2 POWER-ON BASE DRAG	37
4.0	SUMMARY AND CONCLUSIONS	47
5.0	REFERENCES	49
6.0	SYMBOLS AND DEFINITIONS	52
DISTRIBUTION		(1)

ILLUSTRATIONS

Figure		Page
1	NOMENCLATURE FOR POWER-ON CONDITIONS FOR ROCKETS AND BASE BLEED CONCEPTS	3
2	CORRELATION OF AVERAGE BASE PRESSURE FOR SOME CONDITIONS AT EXIT	4
3A	CORRELATION OF BASE PRESSURE RATIO WITH MACH NUMBER FOR THRUST COEFFICIENT TYPICAL OF BOOSTER ROCKET MOTORS (M_j = 1.7 TO 2.7, dj/d_B = 0.8)	7
3B	EXPERIMENTAL BASE PRESSURE COEFFICIENT VS THRUST COEFFICIENT (M_∞ = 2.5, dj/dr = 0.8, CONICAL NOZZLE EXIT)	9
4	ALTERNATIVES TO COMPUTE POWER-ON BASE DRAG IN AP02	14
5	BASE PRESSURE AS A FUNCTION OF I FOR VARIOUS EXIT AREAS AT M_∞ = 3.0 (REFERENCE 15)	16
6	BASE PRESSURE AS A FUNCTION OF I FOR VARIOUS MACH NUMBERS AT dj/dr = 0.4 (REFERENCES 10 AND 3)	16
7	MEAN BODY-ALONE BASE PRESSURE COEFFICIENT USED IN AP98[8]	18
8	MODIFIED EMPIRICAL BASE DRAG PREDICTION MODEL OF REFERENCE 4	19
9A	PERCENT INCREASE IN BODY-ALONE BASE PRESSURE COEFFICIENT DUE TO ANGLE OF ATTACK ($M_\infty \geq 2$)	21
9B	PERCENT INCREASE IN BODY-ALONE BASE PRESSURE COEFFICIENT DUE TO ANGLE OF ATTACK ($M_\infty < 2$)	22

ILLUSTRATIONS (Continued)

Figure		Page
10	PERCENT INCREASE IN BASE PRESSURE COEFFICIENT DUE TO COMBINED EFFECTS OF ANGLE OF ATTACK AND CONTROL DEFLECTION ($t/c \approx 0$)	23
11	PERCENT CHANGE IN BASE PRESSURE COEFFICIENT DUE TO FIN THICKNESS AT VARIOUS VALUES OF $\lvert\alpha + \delta\rvert$	23
12A	PERCENT INCREASE IN BASE PRESSURE COEFFICIENT DUE TO FIN LOCATION ($\lvert\alpha + \delta\rvert = 0$ DEG, $M_\infty = 2.0$)	24
12B	PERCENT INCREASE IN BASE PRESSURE COEFFICIENT DUE TO FIN LOCATION ($\lvert\alpha + \delta\rvert = 5.0$ DEG, $M_\infty = 2.0$)	24
12C	PERCENT INCREASE IN BASE PRESSURE COEFFICIENT DUE TO FIN LOCATION ($\lvert\alpha + \delta\rvert = 10.0$ DEG, $M_\infty = 2.0$)	25
13	COMPARISON OF THEORY AND EXPERIMENT FOR BASE PRESSURE RATIO AT BASE BLEED CONDITIONS ($M_\infty = 1.58$; dj/dr = 0.4; Tj = 520 °R)	28
14	COMPARISON OF THEORY AND EXPERIMENT FOR BASE PRESSURE RATIO AT BASE BLEED CONDITIONS ($M_\infty = 2.0$; dj/dr = 0.4; Tj = 520 °R)	28
15	COMPARISON OF THEORY AND EXPERIMENT FOR BASE PRESSURE RATIO AT BASE BLEED CONDITIONS ($M_\infty = 2.5$; dj/dr = 0.4; Tj = 520 °R)	29
16A	COMPARISON OF THEORY AND EXPERIMENT FOR BASE PRESSURE RATIO AT BASE BLEED CONDITIONS ($M_\infty = 3.0$; dj/dr = 0.4; Tj = 520 °R)	29
16B	UPPER LIMIT OF I VERSUS dj/dr FOR ACCURATE VALUES OF P_B/P_∞	30
17	COMPARISON OF THEORY AND EXPERIMENT FOR BASE PRESSURE RATIO AT BASE BLEED CONDITIONS ($M_\infty = 3.88$; dj/dr = 0.4; Tj = 520 °R)	30

ILLUSTRATIONS (Continued)

Figure		Page
18	COMPARISON OF THEORY AND EXPERIMENT FOR BASE PRESSURE RATIO AT BASE BLEED CONDITIONS ($M_\infty = 0.71$; dj/dr = 0.31; Tj = 2150 °R)	32
19	COMPARISON OF THEORY AND EXPERIMENT FOR BASE PRESSURE RATIO AT BASE BLEED CONDITIONS ($M_\infty = 0.98$; dj/dr = 0.31; Tj = 2150 °R)	32
20	COMPARISON OF THEORY AND EXPERIMENT FOR BASE PRESSURE RATIO AT BASE BLEED CONDITIONS ($M_\infty = 2.0$; dj/dr = 0.2; Tj = 5400 °R)	33
21	REVISED DANBERG[3] MODEL FOR BASE BLEED	34
22A	M864 155 MM PROJECTILE (ALL DIMENSIONS IN CALIBERS)	35
22B	ZERO LIFT DRAG COMPARISONS OF THEORY AND EXPERIMENT FOR 155 MM, M864 PROJECTILE (I = 0)	35
22C	ZERO LIFT DRAG OF M864 PROJECTILE FOR TYPICAL VALUES OF BASE BLEED PARAMETER	36
23	COMPARISON OF THEORY AND EXPERIMENT FOR BASE DRAG AS A FUNCTION OF MASS INJECTION PARAMETER	37
24	COMPARISON OF POWER-ON BASE PRESSURE PREDICTION WITH EXPERIMENT (Mj = 2.0, $M_\infty = 2.0$)	38
25	COMPARISON OF POWER-ON BASE PRESSURE COEFFICIENT PREDICTION WITH EXPERIMENT (Mj = 1, $M_\infty = 2.41$, $dj/d_B = 0.5$)	39
26	COMPARISON OF POWER-ON BASE PRESSURE COEFFICIENT PREDICTION WITH EXPERIMENT (Mj = 1.0, $dj/d_B = 0.45$)	39
27	COMPARISON OF POWER-ON BASE PRESSURE COEFFICIENT PREDICTION WITH EXPERIMENT (Mj = 2.5, $M_\infty = 1.94$, dj/dr = 0.75)	40
28	COMPARISON OF POWER-ON BASE PRESSURE COEFFICIENT PREDICTION WITH EXPERIMENT (Mj = 3.5, $M_\infty = 1.94$, $dj/d_B = 0.75$)	41

ILLUSTRATIONS (Continued)

Figure		Page
29	COMPARISON OF POWER-ON BASE PRESSURE COEFFICIENT PREDICTION WITH EXPERIMENT (M_∞ = 2.5, dj/dr = 0.2)	41
30	COMPARISON OF POWER-ON BASE PRESSURE PREDICTION WITH EXPERIMENT FOR CYLINDRICAL AFTERBODY (Mj = 2.7, dj/d_B = 0.8, 0.45; θj = 20 DEG)	43
31	COMPARISON OF POWER-ON BASE PRESSURE PREDICTION WITH EXPERIMENT FOR BOATTAIL AFTERBODY (dj/dr = 0.45; θj = 20 DEG; θ_B = 6.35 DEG; ℓ_B = 0.82 CAL; Mj = 2.7)	44
32	COMPARISON OF POWER-ON BASE PRESSURE PREDICTION WITH EXPERIMENT FOR FLARE AFTERBODY (Mj = 2.7; dj/dr = 0.8; θj = 20 DEG; θ_B = 6.54 DEG; ℓ_B = 1.34 CAL)	45
33	COMPARISON OF POWER-ON BASE PRESSURE PREDICTION WITH EXPERIMENT FOR A BOATTAILED AFTERBODY (Mj = 2.7; dj/dr = 0.45; θj = 20 DEG)	46

TABLES

Table		Page
1	EMPIRICAL MODEL AND PARAMETERS TO DEFINE POWER-ON BASE PRESSURE	9
2	NEGATIVE BASE PRESSURE COEFFICIENTS $\left(-C_{P_B}\right)$ FOR VARIOUS FLARE ANGLES AS A FUNCTION OF MACH NUMBER	10
3	NEGATIVE BASE PRESSURE COEFFICIENTS $\left(-C_{P_B}\right)$ FOR VARIOUS FLARE ANGLES AS A FUNCTION OF MACH NUMBER	26

1.0 INTRODUCTION

The present approach to predict the effect of the rocket engine burning on the base drag of weapons was integrated into the aeroprediction code in the late 1970's and has not been upgraded since that time. The method utilized was basically an extension of the Brazzel[1] technique by Johnson.[2] The Brazzel technique was for solid rockets, which had an exit Mach number of 1.0 or greater. It required knowledge of some of the details of the rocket such as chamber pressure, exit area to nozzle throat area, specific heat ratio of the exit gas, and location of the nozzle exit with respect to the base of the missile or projectile. This approach has been shown to give reasonable estimates of power-on base drag for a limited range of flight conditions when these parameters (P_C/P_∞, A_j/A_t, γ_j, x_j/d_r) are known.

While the approach by Brazzel has its strengths, it also has several weaknesses when approached from an aerodynamics viewpoint. First, it was limited to jet momentum flux ratios (RMF) of about 2.5 or less. Many of the world's rockets have values of this parameter much higher and therefore the method of Brazzel needs to be extended to higher values of RMF. This was done and documented informally[2] many years ago, but has never been documented formally. This report will serve as formal documentation of the extension of the Brazzel method to higher values of RMF. Another problem with the Brazzel technique from an aerodynamicist's viewpoint is the required knowledge of the engine parameters. These parameters are required in order to perform conceptual design tradeoffs of various rockets for total drag when the engine is burning. As a result of this desire for conceptual trade studies where some account of engine–on base drag is considered, other simplified procedures are needed for base drag prediction. This report will address two other options for the user of the aeroprediction code to calculate power–on base drag when the user knows little about the engine. Another limitation of the Brazzel method is its limitation to supersonic flow at the nozzle exit. While the exit supersonic flow requirement is not a severe limitation for most rocket engines, it is a severe limitation for projectile configurations that use base bleed for base drag reduction. As a result of this shortcoming, a method developed by Danberg[3] for predicting base drag for small values of the bleed injection parameter (I) will be incorporated into the aeroprediction code. A final limitation of the Brazzel method is that it was derived based on freestream Mach number data of 1.5 and greater. It therefore needs to be extended to at least the transonic Mach number regime.

The modifications to the aeroprediction code for power-on base drag prediction will be a part of the next release to the public, which will be in 2002 (AP02). The power-on base drag modifications will also be incorporated into the personal computer interface for the AP02 so as to allow the various power-on options to be considered in a very user friendly mode.

2.0 ANALYSIS

2.1 POWER-ON BASE DRAG FOR $M_j \geq 1.0$

Since the power-on base drag prediction method of the AP98 is based on an extension of the method of Brazzel, et al, it is appropriate to briefly summarize Brazzels method. Figure 1A shows the nomenclature that is used for the rocket engine parameters. As seen in Figure 1A, P_C is the chamber pressure of the rocket which is also the stagnation pressure since velocity of the gas is zero. d_t is the diameter of the nozzle throat and d_j is the nozzle exit diameter. T_j, M_j, γ_j, and P_j are all conditions of the rocket exhaust at the nozzle exit plane. x_j is the distance aft of the base that the nozzle exit plane is located. The base pressure, P_B, is the pressure on the base of the rocket external to the exit plane. The Brazzel and Henderson method defines the base pressure as

$$P_B / P_\infty = \left[\frac{T_j}{T_j^*}\right]\left[0.19 + 1.28\left(\frac{RMF}{1+RMF}\right)\right]\left[\frac{3.5}{1+2.5\left(d_B/d_r\right)^2}\right] + 0.047\left(5 - M_\infty\right)\left[2\left(x_j/d_B\right) + \left(x_j/d_B\right)^2\right] \quad (1)$$

where $$RMF = \frac{\gamma_j P_j d_j^2 M_j^2}{\gamma_\infty P_\infty d_r^2 M_\infty^2} \quad (2)$$

$$\frac{T_j}{T_j^*} = \frac{\frac{\gamma_j + 1}{2}}{1 + \frac{\gamma_j - 1}{2} M_j^2} \quad (3)$$

RMF of Equation (2) is defined as the jet momentum flux ratio.

Brazzel's method was built around two fundamental assumptions that he was able to develop based on analysis of experimental data for jet exit Mach numbers 1.0 to 3.8. The first assumption is that freestream Mach number and nozzle diameter are accounted for by the momentum flux term defined by Equation (2). The second assumption was that jet exit Mach number could be described by the ratio of the jet static temperature for a given jet Mach number to that at a jet exit Mach number of 1.0. This relationship is defined by Equation (3).

In reality, the Brazzel method was geared primarily to accounting for base drag for sustainer rocket motors that typically have values of thrust coefficient of 0.2 to about 3.0 and fly supersonically. However, as the mass flow ratio or thrust coefficient get large or the freestream Mach number is transonic, the Brazzel method produces increasingly erroneous results for many cases. This behavior of Equation (1) is illustrated in Figure 2, which correlates base pressure

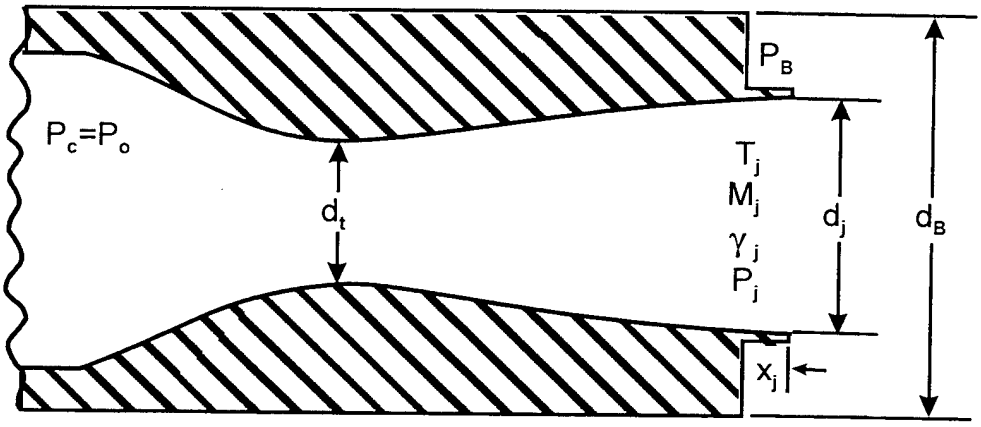

A) ROCKET ENGINE PARAMETERS

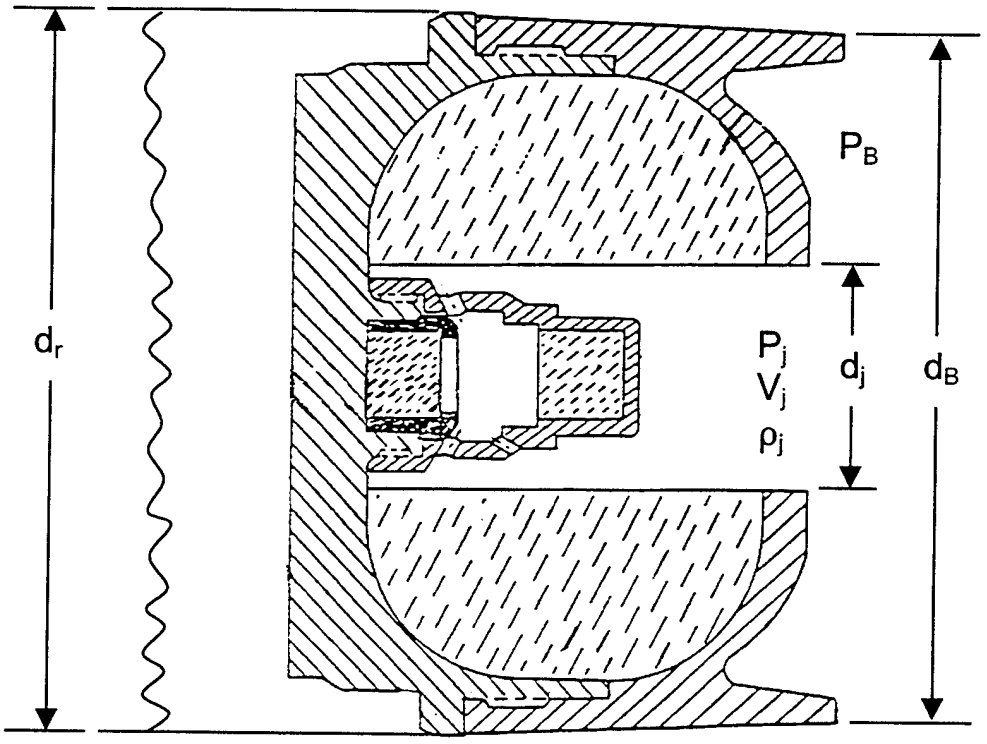

B) A TYPICAL PROJECTILE BASE BLEED CONFIGURATION[3]

FIGURE 1. NOMENCLATURE FOR POWER-ON CONDITIONS FOR ROCKETS AND BASE BLEED CONCEPTS

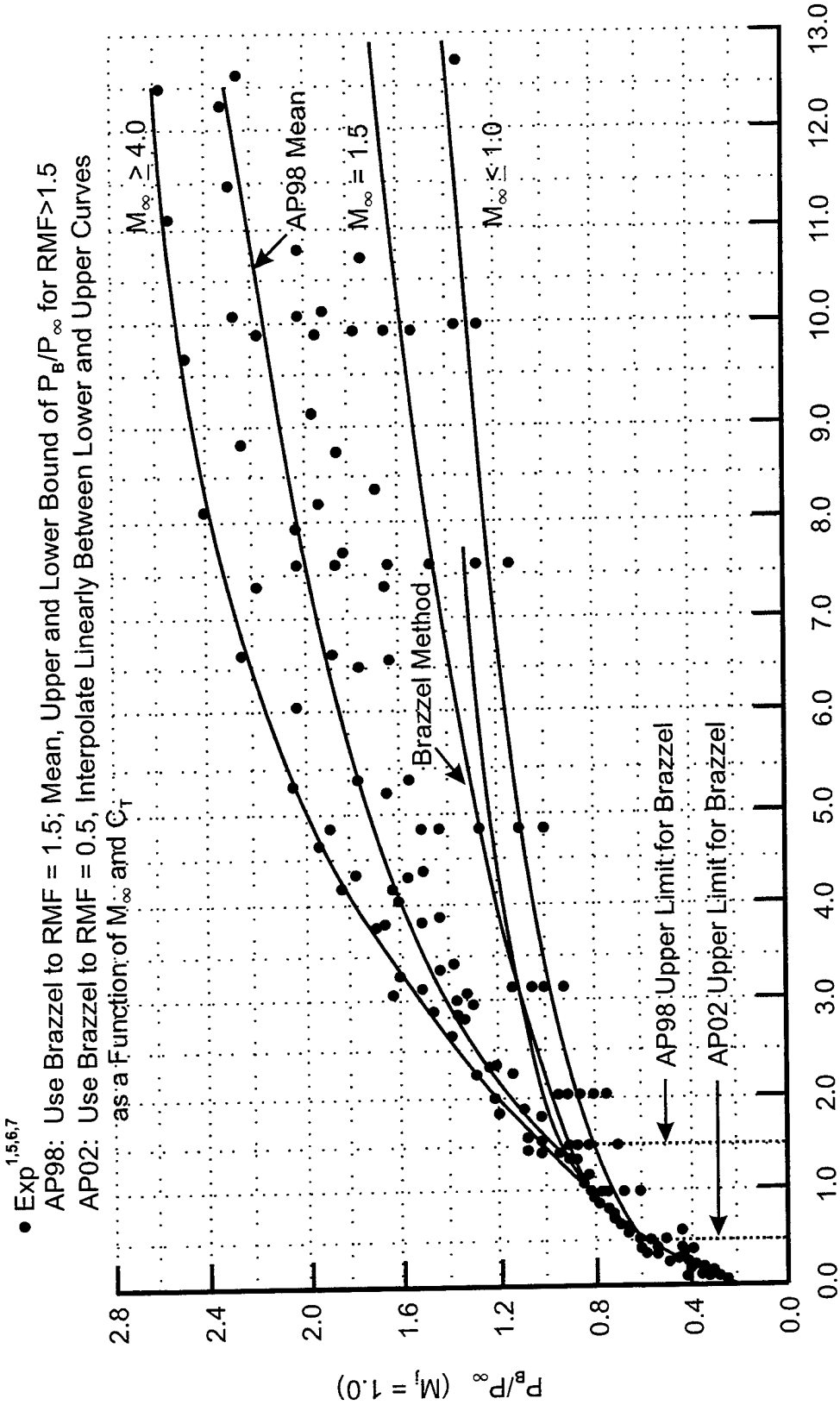

FIGURE 2. CORRELATION OF AVERAGE BASE PRESSURE FOR SOME CONDITIONS AT EXIT

predictions on a cylindrical afterbody for a jet exit Mach number of one $\left(T_j / T_j^* = 1.0\right)$. Note that the Brazzel correlation fits the data taken from references 1, 5, and 6 quite nicely for RMF values up to almost 0.5. Above values of 0.5 the data of Figure 2 is more scattered, particularly for RMF values above about 1.5.

Brazzel indicated he had little data for high thrust ratios to use in the method development. The method of References 2 and 4, and included in the AP98, uses the method of Brazzel for RMF values up to 1.5 and then the empirical curve fits that bracket most of the data of Figure 2 in terms of upper and lower values along with a mean value. This mean value is shown in Figure 2. However, in examining the data of Figure 2 more closely, it was found that for higher values of C_T, P_B/P_∞ was primarily dependent on freestream Mach number with little dependence on jet exit Mach number or jet exit diameter. Apparently, for high thrust levels such as would occur on a high impulse sustainer or a booster rocket motor, one of the main correlation parameters for P_B/P_∞ is M_∞. Thus, the AP02 will modify the current methodology for power on base drag prediction of Reference 4 for RMF values greater than 0.5 so that P_B/P_∞ will be correlated with freestream Mach number, as opposed to giving the user an upper, lower, and mean value of P_B/P_∞ for all freestream Mach numbers. The discussion of power-on base drag prediction will thus be broken down by thrust or momentum flux ratio level.

We will first of all consider the lower values of RMF or C_T which are more representative of a lower thrust sustainer engine. For these values of RMF, we will use the Brazzel method given by Equations (1) through (3). To utilize the Brazzel method, we therefore must obtain values of RMF either through direct input or through calculation based on known engine quantities. The parameters that are normally known in a rocket engine are the chamber pressure, P_C, the nozzle throat and exit area and the ratio of specific heats for the gas of interest. We can use this information to determine the quantities M_j and RMF through the following process. We will first of all assume isentropic flow throughout the nozzle. This means there are no strong shock waves in the nozzle, only weak expansion or compression waves. This means that the chamber pressure, which is the total pressure, is constant throughout the nozzle (since velocity is zero in the chamber). Thus

$$\frac{P_C}{P_\infty} = \frac{P_O}{P_\infty} = \left(\frac{P_{O_j}}{P_j}\right)\left(\frac{P_j}{P_\infty}\right) \tag{4}$$

Also for isentropic flow, the nozzle exit to throat area ratio can be related to the exit Mach number through the expression[4]:

$$\frac{A_j}{A_t} = \frac{1}{M_j}\left[\left(\frac{2}{\gamma_j + 1}\right)\left(1 + \frac{\gamma_j - 1}{2} M_j^2\right)\right]^{\frac{\gamma_j + 1}{2(\gamma_j - 1)}} \tag{5}$$

Knowing d_j, d_t, and γ_j, Equation (5) can be solved iteratively using something like the Newton-Raphson method for the exit Mach number M_j. Knowing M_j, then since,

$$\frac{P_{O_j}}{P_j} = \left[1 + \frac{\gamma_j - 1}{2} M_j^2\right]^{\frac{\gamma_j}{\gamma_j - 1}} \tag{6}$$

The exit pressure P_j can be determined since P_{O_j} is known from P_C. That is

$$P_j = P_{O_j}\left[1 + \frac{\gamma_j - 1}{2} M_j^2\right]^{-\left(\frac{\gamma_j}{\gamma_j - 1}\right)}$$

or

$$\frac{P_j}{P_\infty} = \frac{P_C}{P_\infty}\left[1 + \frac{\gamma_j - 1}{2} M_j^2\right]^{-\left(\frac{\gamma_j}{\gamma_j - 1}\right)} \tag{7}$$

Now knowing P_j/P_∞, A_j/A_{ref}, M_j/M_∞ and γ_j/γ_∞, we can compute the jet momentum flux ratio from Equation (2). Finally, knowing x_j/x_B and T_j/T_j^* from Equation (3), the base pressure ratio for power on can be computed from Equation (1).

The base pressure coefficient is defined by

$$C_{P_B} = \frac{2}{\gamma M_\infty^2}\left[\frac{P_B}{P_\infty} - 1\right] \tag{8}$$

where P_B/P_∞ comes from Equation (1). Finally, the base drag coefficient for power on conditions is

$$C_{A_B} = -C_{P_B}\left[\left(\frac{d_B}{d_r}\right)^2 - \left(\frac{d_j}{d_r}\right)^2\right] \tag{9}$$

Also notice that Equation (9) subtracts out that part of the base area attributed to the jet exit diameter, where the pressure is P_j, not P_b. P_j is used in the calculation of jet thrust coefficient through the relationship

$$C_T = 2\,RMF + \left(\frac{d_j}{d_r}\right)^2 \frac{2}{\gamma_\infty M_\infty^2}\left(\frac{P_j}{P_\infty} - 1\right) \tag{10a}$$

Of course, thrust coefficient is also related to the thrust through the nondimensional equation

$$C_T = \frac{2T}{\gamma_\infty P_\infty M_\infty^2 A_{ref}} \tag{10b}$$

RMF and P_j/P_∞ of Equation (10a) come from Equations (2) and (7), respectively. The total axial force coefficient is then

$$C_A = C_{A_W} + C_{A_f} + C_{A_B} - C_T \tag{10c}$$

where C_{A_W}, C_{A_f}, and C_{A_B} are the axial force coefficients due to wave, skin-friction, and base drag, respectively.

As mentioned earlier, Equation (1) is limited to low to moderate values of jet momentum flux ratio (RMF $\leq$ 0.5). Many rockets, including some in the Navy, have values of RMF much higher than 0.5. As a result, the method of Brazzel, et al,[1] was extended to higher values of RMF using data later taken by Craft and Brazzel,[5] Henderson,[6] and Deep, et al.[7]

Figure 3A is a summary of the data of Reference 6 which varies jet exit Mach number from 1.7 to 2.7 and varies jet to reference diameter from 0.8 to 0.93. Figure 3A is plotted as a function of thrust coefficient.

Thrust, or thrust coefficient, is more likely known for rocket motors as opposed to jet momentum flux ratio, which must be calculated. Hence, this is the parameter on which Figure 3A is based. As seen in Figure 3A, as C_T gets large, the base drag ($P_B/P_\infty < 1.0$) becomes a base thrust ($P_B/P_\infty > 1.0$).

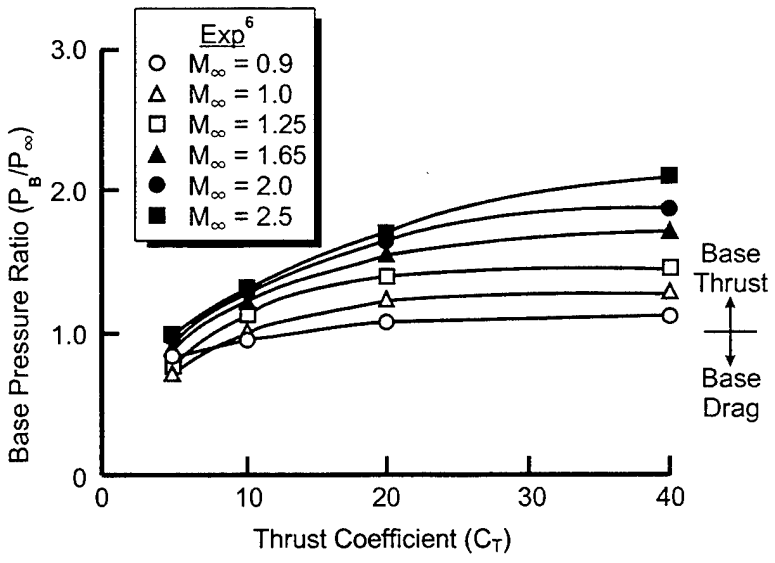

FIGURE 3A. CORRELATION OF BASE PRESSURE RATIO WITH MACH NUMBER FOR THRUST COEFFICIENTS TYPICAL OF BOOSTER ROCKET MOTORS (Mj = 1.7 TO 2.7, dj/d_B = 0.8)

Also, Figure 3A illustrates that for high values of C_T, jet exit Mach number is not as important a parameter since exit Mach number varied from 1.7 to 2.7 for this set of data. Little variation was found in the data of Reference 6 versus exit Mach number, so a mean curve was drawn through the experimental data for each freestream Mach number.

Figure 3B presents a summary of the data from Reference 7 for high values of thrust coefficient for various nozzle geometries at $M_\infty = 2.5$. As seen in Figure 3B, nozzle exit Mach number and geometry play a large role in base pressure ratio. This contradiction in Figure 3A and 3B was one reason the AP81, and all more recent versions of the aeroprediction code, gave a lower, upper, and mean value of power-on base pressure coefficient for various values of RMF or C_T (see Figure 2). Also shown on Figure 3B for comparison purposes is the single curve from Figure 3A based on the Reference 6 data at $M_\infty = 2.5$. This data was taken for jet exit Mach numbers of 1.7 to 2.7 and for conical exit angles of 9.1 deg to 23.3 deg. In fact, the $\theta_j = 9.1$, $M_j = 2.7$ condition is very nearly the same as the $\theta_j = 10$ deg, $M_j = 2.7$ condition of the Reference 5 data. Note the large difference in the data of References 5 and 6 for this condition. On the other hand, the Reference 6 data and Reference 5 data for the $M_j = 2.0$, $\theta_j = 10$ deg and $M_j = 2.7$ and $\theta_j = 20$ deg conditions are fairly consistent. The authors cannot explain the inconsistency in the data of References 5 and 6. One is left with the conclusion that there are some physics going on that require conditions other than M_∞, M_j, θ_j, d_j/d_r, γ_j, γ_∞ to be accounted for, or some of the data in Reference 5 had measurement problems. Some possible sources of inconsistencies between the Reference 5 and 6 data are boundary layer separation at the aft of the body where the plume and freestream meet, laminar versus turbulent conditions at the aft end, which can affect base pressure, or the bow shock reflecting off the tunnel wall in the base region. At any rate, the authors will use Figure 3A as the model for base pressure in the AP02. In so doing, the authors recognize that the empirical model that will be a part of the AP02 may not account for some of the physics going on at the base of the configuration in some cases. However, the preponderance of the experimental data the authors have examined seems to imply that as freestream Mach number and thrust coefficient increase, the base pressure ratio increases in analogy to Figure 3A,versus the lower curves in Figure 3B.

The method that will be a part of the AP02 will therefore have several changes from that in the AP98. First, the method of Brazzel will be used up to values of RMF of 0.5 versus 1.5 as currently done in the AP98. Next, for values of RMF > 0.5, a more robust empirical relationship was derived for P_b/P_∞ than Equation (1). This equation is defined by

$$P_b/P_\infty = \left[\frac{T_j}{T_j^*}\right]^N \left[C_1(C_T, M_\infty) + C_2(M_\infty)\left(\frac{RMF}{1+RMF}\right)\right] f(d_B/d_r) + 0.047(5 - M_\infty)\left[2(x_j/d_B) + (x_j/d_B)^2\right] \quad (11a)$$

where

$$N = \frac{12 - C_T}{11.0}, \quad 1.0 \le C_T < 12$$
$$= 0, \quad C_T \ge 12$$
$$= 1, \quad C_T < 1.0$$

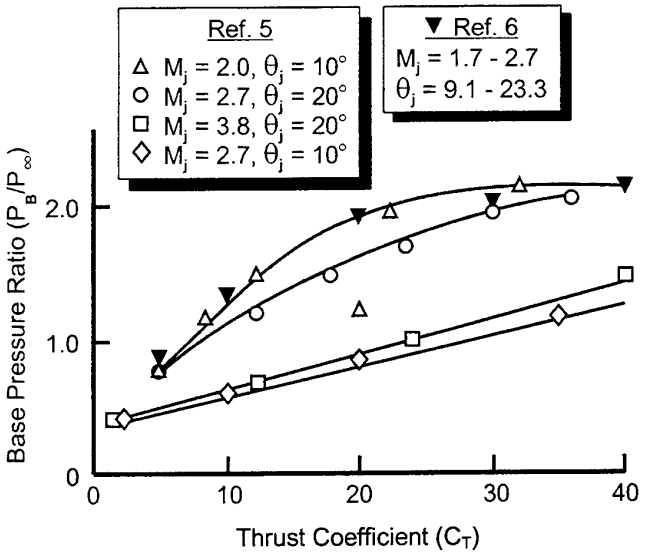

FIGURE 3B. EXPERIMENTAL BASE PRESSURE COEFFICIENT VS THRUST COEFFICIENT (M_∞ = 2.5, dj/dr = 0.8, CONICAL NOZZLE EXIT)

C_1 (C_T, M_∞) and C_2 (M_∞) of Equation (11a) are found from Table 1 by linearly interpolating based on a given value of C_T and M_∞. Also, for Mach numbers below about 1.5, it was found that T_j / T_j^* should have limiting lower values. This limiting lower value is defined by

$$\left(T_j/T_j^*\right)_{min} = 0.7 - \left(M_\infty - 1.2\right)\frac{\left(0.7 - T_j/T_j^*\right)}{0.3}; 1.2 \le M_\infty < 1.5$$
$$\left(T_j/T_j^*\right)_{min} = 0.7 \qquad ; M_\infty < 1.2 \qquad (11b)$$

TABLE 1. EMPIRICAL MODEL AND PARAMETERS TO DEFINE POWER-ON BASE PRESSURE

M_∞	C_1 (C_T, M_∞)					C_2 (M_∞, C_T)	
	C_T					C_T	
	≤1.0	2.0	20	40	≥70	≤1.0	≥2.0
≤0.9	0.19	0.16	-0.06	0.02	0.0	1.24	1.24
1.0	0.19	-0.085	-0.06	0.02	0.0	1.28	1.37
1.25	0.19	-0.085	-0.01	0.02	0.0	1.28	1.47
1.65	0.19	-0.175	-0.06	0.04	0.0	1.28	1.70
2.0	0.19	-0.30	-0.20	0.02	0.0	1.28	1.90
2.5	0.19	-0.45	-0.23	0.01	0.0	1.28	2.30
3.0	0.19	-0.55	-0.22	-0.03	0.0	1.28	2.50
≥4.0	0.19	-0.65	-0.10	-0.04	0.0	1.28	2.7

NSWCDD/TR-00/67

Equations (1) – (10), except Equation (11) is substituted for Equation (1). If thrust and P_j/P_∞ are given, then from Equation (10),

$$RMF = \frac{1}{2}\left[C_T - \left(\frac{d_j}{d_r}\right)^2 \frac{2}{\gamma_\infty M_\infty^2}\left(\frac{P_j}{P_\infty} - 1\right)\right] \tag{12a}$$

Then utilizing Equation (2)

$$M_j = \sqrt{\frac{RMF\ \gamma_\infty\ P_\infty\ d_r^2\ M_\infty^2}{\gamma_j\ P_j\ d_j^2}} \tag{12b}$$

Likewise, if thrust and M_j are known, then utilizing Equations (2) and (10) we obtain

$$\frac{P_j}{P_\infty} = \frac{C_T + \frac{2}{\gamma_\infty M_\infty^2}\left(\frac{d_j}{d_r}\right)^2}{\frac{2}{\gamma_\infty M_\infty^2}\left(\frac{d_j}{d_r}\right)^2\left[1+\gamma_j M_j^2\right]} \tag{13}$$

RMF can then be computed from Equation (2).

Finally, if thrust and P_C/P_∞ are given then utilizing Equations (13), (4), and (6), we obtain:

$$\frac{P_C}{P_\infty} = \frac{\left[C_T + \frac{2}{\gamma_\infty M_\infty^2}\left(\frac{d_j}{d_r}\right)^2\right]\left[1+\frac{\gamma_j - 1}{2} M_j^2\right]^{\frac{\gamma_j}{\gamma_j - 1}}}{\frac{2}{\gamma_\infty M_\infty^2}\left(\frac{d_j}{d_r}\right)^2\left[\gamma_j M_j^2 + 1\right]} \tag{13a}$$

All terms in Equation (13a) are known except M_j. M_j can be found by a numerical iterative solution of Equation (13a).

Of course, C_T is defined by Equation (10b) repeated here for convenience:

$$C_T = \frac{2T}{\gamma_\infty P_\infty M_\infty^2 A_{ref}} \tag{14}$$

C_{P_B}, C_{A_B}, and C_A are then obtained through use of Equations (8), (9), and (10), respectively.

A third alternative for rocket engine effects on base drag and total weapon performance is where you know nothing about the rocket engine, except you know you want to parametrically trade off power-on base drag conditions as a function of the key engine parameters. To do this we will assume several alternatives. The first assumes $C_{A_B} = 0$. For $C_{A_B} = 0$, either $d_j/d_B = 1.0$ or RMF is high enough so that $P_B/P_\infty = 1$. The second alternative is to assume

$$C_{A_B} = \left(C_{A_B}/2\right)_{\text{power off}} \tag{15}$$

This assumption assumes the power-on base drag is half of the power-off value, and is not an unreasonable assumption for many rocket engines with moderate thrust levels. The third assumption assumes

$$C_{A_B} = \left(C_{A_B}\right)_{\text{power off}} \tag{16}$$

That is, Equation (16) says the engine has no effect on base drag. The final alternative is to assume we have a very high value of RMF so that we have a base thrust as opposed to a base drag. For this option we let

$$C_{A_B} = -K\left(C_{A_B}\right)_{\text{power off}} \tag{17}$$

where K varies from -1.5 to 2.5.

While it is true these four alternatives of base drag that allow a variation in C_{A_B} from 1.5 to $-2.5C_{A_B}$ are just approximations based on no real rocket engine, the options are reasonable boundaries of what one should expect for power-on effects on base drag.

Figure 4 summarizes the alternatives to compute power-on base drag that will be a part of the AP02.

2.2 BASE BLEED

Base bleed is an alternative considered for use, primarily in unguided projectiles, to decrease base drag. The concept works on the basis of burning a small amount of propellant in the base of a projectile. This burning generates an exhaust gas which is typically subsonic and incompressible and raises the temperature and pressure in the base area, thus lowering the base drag. Figure 1B is an example of a base bleed configuration taken from Reference 3. There have been numerous references in the literature over the past 40 years or so that address the base bleed problem. Some of the more notable references are given by 9-19, in addition to Reference 3. However, as noted by Danberg[3], many of these references investigated the effects of base bleed or base pressure in wind tunnel tests where fairly high values of the nondimensional injection parameter were used. This parameter is defined by

Option 1 Use Brazzel, et al[1] method for RMF values equal to or less than 0.5.

Inputs Required: $(\text{RMF} \le 0.5 \text{ or } C_T \le 1.0)$

- Chamber pressure ratio (P_C/P_∞)
- Nozzle throat to nozzle exit area ratio
- Nozzle exit diameter
- Nozzle exit location with respect to base
- Specific heat of gas at exit

Option 2 Use modified method of Brazzel for values of RMF > 0.5 or $C_T \ge 1.0$

Inputs Required:

- Thrust
- Specific heat of gas at exit
- Either P_C/P_∞, P_j/P_∞, or M_j
- Nozzle exit location with respect to base
- Nozzle exit diameter

Option 3 No engine parameters known; want to perform conceptual design study for a range of power-on conditions. (k = −1.5 represents the outer boundary of thrust produced from a high thrust booster rocket and k = +2.5 represents the outer boundary of base drag obtained from a low thrust sustainer motor. Most engines fall in between these two extremes.)

Inputs Required: (Select one of the following options)

a) $C_{A_B} = 0$; b) $C_{A_B} = \left(C_{A_B}/2\right)_{\text{power off}}$; c) $C_{A_B} = \left(C_{A_B}\right)_{\text{power off}}$

d) $C_{A_B} = -K\left(C_{A_B}\right)_{\text{power off}}$ with $-1.5 \le K \le 2.5$;

FIGURE 4. ALTERNATIVES TO COMPUTE POWER-ON BASE DRAG IN AP02

$$I = \frac{\dot{m}_j}{\rho_\infty V_\infty A_{ref}} \tag{18}$$

and is the ratio of the mass flow out of the bleed exit to that in a stream tube of area equal to the cross sectional area of the body. Many of the References 9–19 were for wind tunnel tests where values of I = .01 to .04 were considered for cold air whereas the practical case for projectiles is I ≅ .001 to .005 with hot gas. These low values of I for projectiles are due to the fact that only so much propellant can be carried in the projectile cavity (see Figure 1), and if a high value of I is used, the time over which the base drag reduction occurs will be very short. A slower burn, lower velocity exhaust gas, and hence lower value of I is thus more practical, even though the optimum value of I is about .01 to .03 for minimum base drag based on the cold gas tests of References 9 and 10.

Assuming values of I of .001 to .005 allows some simplifications in the base pressure estimation process. This is because for values of $I \le 0.005$, the base pressure is approximately a linear variation with I. This is illustrated by the results of Reference 15 in Figure 5 and of Reference 10 in Figure 6. Figure 5 shows P_b/P_∞ varies nearly linearly for low values of I at $M_\infty = 3.0$ for various injector areas. Figure 6 shows P_b/P_∞ varies nearly linearly for low values of I where $d_j/d_r = 0.4$ and for several values of Mach number. Reference 13 and several other references have also come to the same conclusion of the linear variation of P_b/P_∞ for low values of I typical of base bleed conditions.

Danberg[3] used the conclusion of near linearity of P_b/P_∞ as a function of I for $I < 0.005$ to derive a semiempirical relationship to predict base pressure. Since the purpose of including base bleed in the aeroprediction code (APC) is to allow application primarily to unguided projectiles and since the range of practical interest of base bleed for projectiles is fairly low, a slightly modified method of Danberg will be adopted for use in the APC. Danberg's method defines the base pressure as

$$\frac{P_B}{P_\infty} = \left(\frac{P_B}{P_\infty}\right)_{I=0} + \frac{\sigma I}{1+\beta\sigma I} \tag{19}$$

where

$$\sigma = \frac{d\left(P_b/P_\infty\right)}{dI} = \left[-5.395 + 0.0172T_j\right]M_\infty + \left[4.610 - 0.0146T_j\right]M_\infty^2 + \left[-0.566 + 0.00446T_j\right]M_\infty^3 \tag{20a}$$

and

$$\beta = 15.1 - 46.3\left(M_\infty - 0.71\right) \tag{20b}$$

T_j of Equation (20) must be in degrees Rankine. Also, if β is less than 2.6, it should be set to 2.6 according to Danberg. Also, an upper limit of P_B/P_∞ of 1.0 will be included in the modified Danberg theory. Notice that Equation (19) has some nonlinearity brought into the method through the second term. Danberg used a combination of computational fluid dynamics

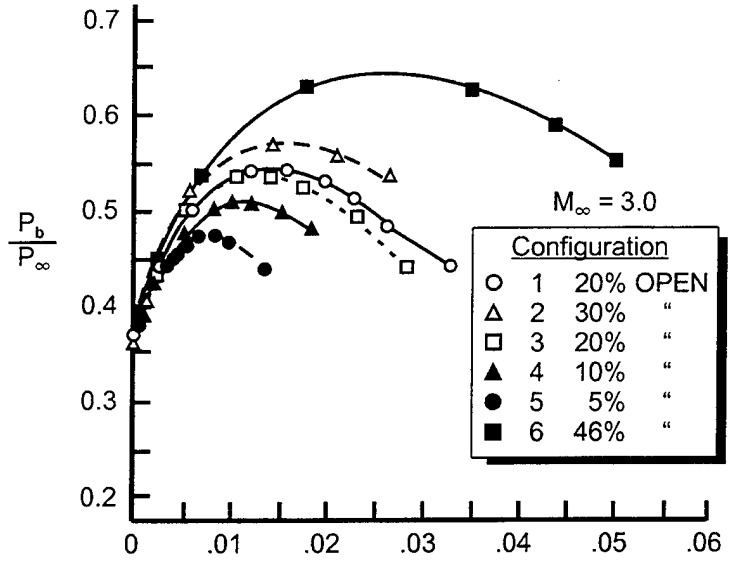

FIGURE 5. BASE PRESSURE AS A FUNCTION OF I FOR VARIOUS EXIT AREAS AT $M_\infty = 3.0$ (REFERENCE 15)

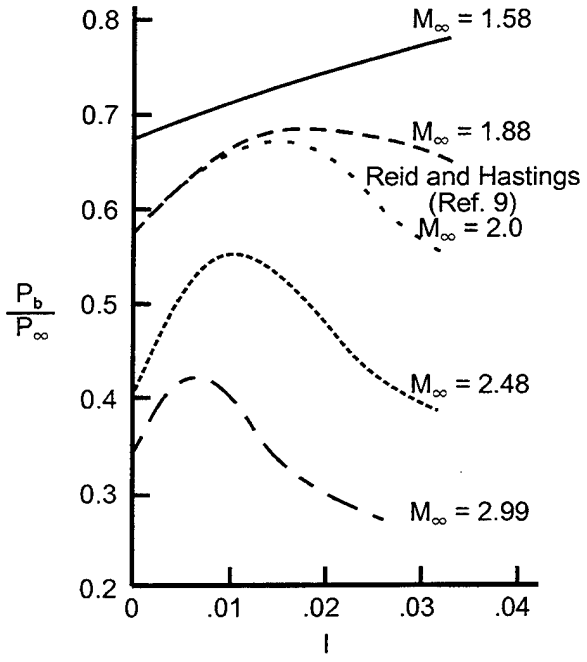

FIGURE 6. BASE PRESSURE AS A FUNCTION OF I FOR VARIOUS MACH NUMBERS AT dj/dr = 0.4 (REFERENCES 10 AND 3)

calculations for forebody wave and skin friction drag, in conjunction with total axial force from ballistic range data, to back out the base axial force term. Knowing C_{A_B}, the base pressure for no base bleed can be calculated from

$$\left(\frac{P_b}{P_\infty}\right)_{I=0} = \frac{\gamma_\infty M_\infty^2}{2} C_{P_B} + 1 \tag{21}$$

Equation (21) is then used as the first term of Equation (19). The present approach differs from Danberg's approach in that $(P_b/P_\infty)_{I=0}$ will be defined based on the present method in the APC.[4] In this approach, a mean base pressure coefficient curve has been defined based on an extensive database taken over many years. This mean base pressure coefficient curve is shown in Figure 7. Thus for a given freestream Mach number, one determines a value of $(P_b/P_\infty)_{I=0}$ from Equation (21). Then for a given value of exit temperature, T_j, freestream Mach number and injection parameter I, the base pressure can be calculated from Equation (19). Base pressure coefficient is then calculated from Equation (8).

For the base bleed methodology, Danberg assumed that $P_j = P_B$ in his analysis. Hence, for base bleed, we do not subtract the area of the exit from the axial force calculations as we did for rocket motors (see Equation 9). The base axial force coefficient for base bleed conditions is thus

$$C_{A_B} = -C_{P_B}\left(\frac{d_B}{d_r}\right)^2\left(\frac{d_B}{d_r}\right)^i \quad \begin{array}{l} ; i = 0 \text{ for flare} \\ ; i = 1 \text{ for boattail} \end{array} \tag{22}$$

To summarize the new methodology which will be incorporated into the 2002 version of the aeroprediction code, we will use a slightly modified method of Danberg where base pressure is defined by Equations (19), (20), and Figure 7; and base axial force by Equation (22). Equation (19) requires an input value of freestream Mach number, exit temperature in degrees Rankine and a value of the Injection parameter I. For most accuracy, I should be less than 0.005, but values of I as high as 0.01 can be assumed, but with larger errors in the prediction process.

2.3 MODIFIED BASE DRAG PREDICTION MODEL

The base drag prediction model currently in use in the AP98 is described in References 4 and 8. This model accounts approximately for the effects of Mach number, angle of attack, fin thickness, fin location, fin local angle of attack, power-on/off, and boattail or flare. A slight modification to the method of Reference 4 is being made here as a result of Equation (9), which excludes the jet area for rockets, whereas for base bleed, the jet area is included. The modified base drag computational process is summarized in Figure 8.

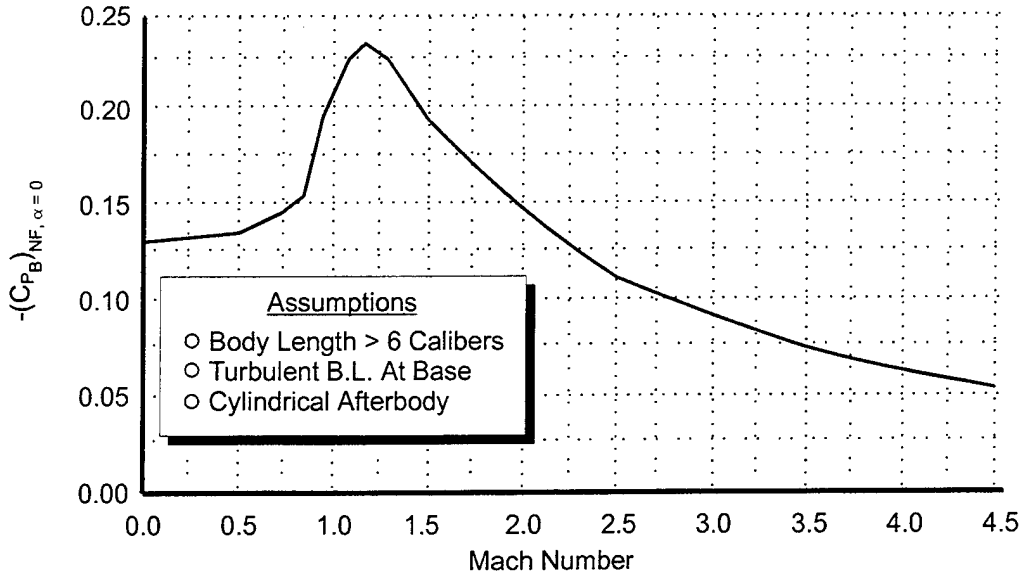

FIGURE 7. MEAN BODY-ALONE BASE PRESSURE COEFFICIENT USED IN AP98[8]

The first step in Figure 8 is to compute the body alone effects on base pressure coefficient due to Mach number and angle of attack. The base pressure coefficient of the body alone at zero angle of attack as a function of Mach number is shown in Figure 7. The factor F, of Equation (1) in Figure 8 is defined in Figure 9A for $M_\infty \geq 2.0$ and in Figure 9B for $M_\infty < 2.0$. These results were taken directly from Reference 4. The reader is referred to that reference for the derivation of these figures as well as the overall base drag prediction model in the AP98.[8]

Part B of Figure 8 treats the effect of tail fins on the base pressure coefficient. There are three effects accounted for empirically in Reference 4 and Figure 8. These are fin thickness and local angle of attack effects, which are defined by Equation (2) of Figure 8, and fin location effects, which are defined by Equation (8) of Figure 8. F_2 and F_3 of Equation (2) of Figure 8 is defined by Figures 10 and 11, respectively. Figure 10 shows that there can be a fairly substantial increase in the power off base pressure coefficient as the local angle of attack of the wing is increased. Figure 11 shows the additional increase in the magnitude of C_{P_B} due to fin thickness effects. It is seen that this effect is the largest when $|\alpha + \delta| = 0$ and goes to zero when $|\alpha + \delta| \geq$ 30 deg. In other words, when one has a fairly large local angle of attack on the wing, Figure 10 shows the magnitude of the base pressure coefficient increasing, but additional effects due to thickness (Figure 11) are reduced over what they would be if the local angle of attack were zero.

The final fin effect on Figure 8 is the fin location effect, which is defined by Equation (3) of Figure 8. Note that both Figures 10 and 11 were derived with fins located flush with the base of the projectile or missile. Figures 12A, 12B, and 12C show the effect of various fin thickness to body reference diameter on base pressure as a function of fin location, all at $M_\infty = 2.0$. Figure 12A is for $|\alpha + \delta| = 0$ deg, Figure 12B is for $|\alpha + \delta| = 5$ deg, and Figure 12C is for $|\alpha + \delta| = 10$ deg. Referring to Equation (3) of Figure 8, the first term of Equation (3) is the

A. Body Alone C_{P_B}

1. Compute $\left(C_{P_B}\right)_{NF,\alpha=0}$ based on data base of C_{P_B} vs M_∞ (see Figure 7)

2. Base Bleed (Inputs: I, T_j)

$$P_B/P_\infty = \frac{\gamma_\infty M_\infty^2}{2}\left(C_{P_B}\right)_{NF,\alpha=0} + 1 + \frac{\sigma I}{1+2.6\sigma I} \tag{1}$$

$$\left(C_{P_B}\right)_{NF,\alpha=0} = \frac{2}{\gamma M_\infty^2}\left[\frac{P_B}{P_\infty} - 1\right] \tag{2}$$

3. Power-On: Brazzel (inputs: P_C/P_∞, A_T/A_j, x_j/d_r, γ_j)

- $$P_B/P_\infty = \frac{T_j}{T_j^*}\left[0.19 + 1.28\left(\frac{RMF}{1+RMF}\right)\right]\left[\frac{3.5}{1+2.5\left(d_B/d_r\right)^2}\right] + 0.047\left(5-M_\infty\right)\left[2\left(x_j/d_B\right)+\left(x_j/d_B\right)^2\right] \tag{3}$$

- Compute C_{P_B} from Equation (2)

4. Power-on: Modified Brazzel (Inputs: T, d_j/d_r, γ_j, x_j/d_r, and either P_C/P_∞, P_j/P_∞ or M_j)

- $$P_B/P_\infty = \left(\frac{T_j}{T_j^*}\right)^N\left[C_1\left(C_T,M_\infty\right)+C_2\left(C_T,M_\infty\right)\left(\frac{RMF}{1+RMF}\right)\right]\left[\frac{3.5}{1+2.5\left(d_B/d_r\right)^2}\right] + 0.047\left(5-M_\infty\right)\left[2\left(x_j/d_B\right)+\left(x_j/d_B\right)^2\right] \tag{4}$$

- Compute C_{P_B} from Equation (2)

5. Power-on: Conceptual Design

- $$C_{A_B} = f\left[\left(C_{A_B}\right)_{\text{power off}}\right] \quad ; \quad f = -1.5 \text{ to } 2.5 \tag{5}$$

FIGURE 8. MODIFIED EMPIRICAL BASE DRAG PREDICTION MODEL OF REFERENCE 4

B. Body Alone α Effects

$$\left(C_{P_B}\right)_{NF,\alpha} = \left(C_{P_B}\right)_{NF,\alpha=0}\left[1 + 0.01\,F_1\right] \tag{6}$$

F_1 = Body Alone α Effects (see Figure 9)

C. Tail Fin Effects

1. Deflection and Thickness Effects

$$\left(C_{P_B}\right)_{\alpha,\delta,t/c,x/c=0} = \left(1 + 0.01\,F_2\right)\left(C_{P_B}\right)_{NF,\alpha=0} + 0.01\,F_3\left(t/d\right) \tag{7}$$

$F_2 = |\alpha + \delta|$ Effects (see Figure 10)

F_3 = Additional Effects due to Thickness (see Figure 11)

2. Fin Location Effects when x/c ≠ 0

$$\left(C_{P_B}\right)_{\alpha,\delta,t/c,x/c} = \left(C_{P_B}\right)_{NF,\alpha} + 0.01\left(\Delta C_{P_B}\right)_{\alpha,\delta,t/c,x/c=0} \text{ (see Figure 12)} \tag{8}$$

D. Boattail Effect

$$\begin{aligned} C_{A_B} &= -\left(C_{P_B}\right)_{\alpha,\delta,t/c,x/c}\left(d_B/d_r\right)^3 ; \text{ base bleed or power off} \\ &= -\left(C_{P_B}\right)_{\alpha,\delta,t/c,x/c}\left[\left(d_B/d_r\right)^2 - \left(d_j/d_r\right)^2\right]; \text{ power on} \end{aligned} \tag{9}$$

E. Flare Effect

$$\begin{aligned} C_{A_B} &= -\left(C_{P_B}\right)_f\left(d_B/d_r\right)^2 ; \text{ base bleed or power off} \\ &= -\left(C_{P_B}\right)_{\alpha,\delta,t/c,x/c}\left[\left(d_B/d_r\right)^2 - \left(d_j/d_r\right)^2\right]; \text{ power on} \end{aligned} \quad ; \text{ see Table 3 for } \left(C_{P_B}\right)_f \tag{10}$$

FIGURE 8. MODIFIED EMPIRICAL BASE DRAG PREDICTION MODEL OF REFERENCE 4 (Continued)

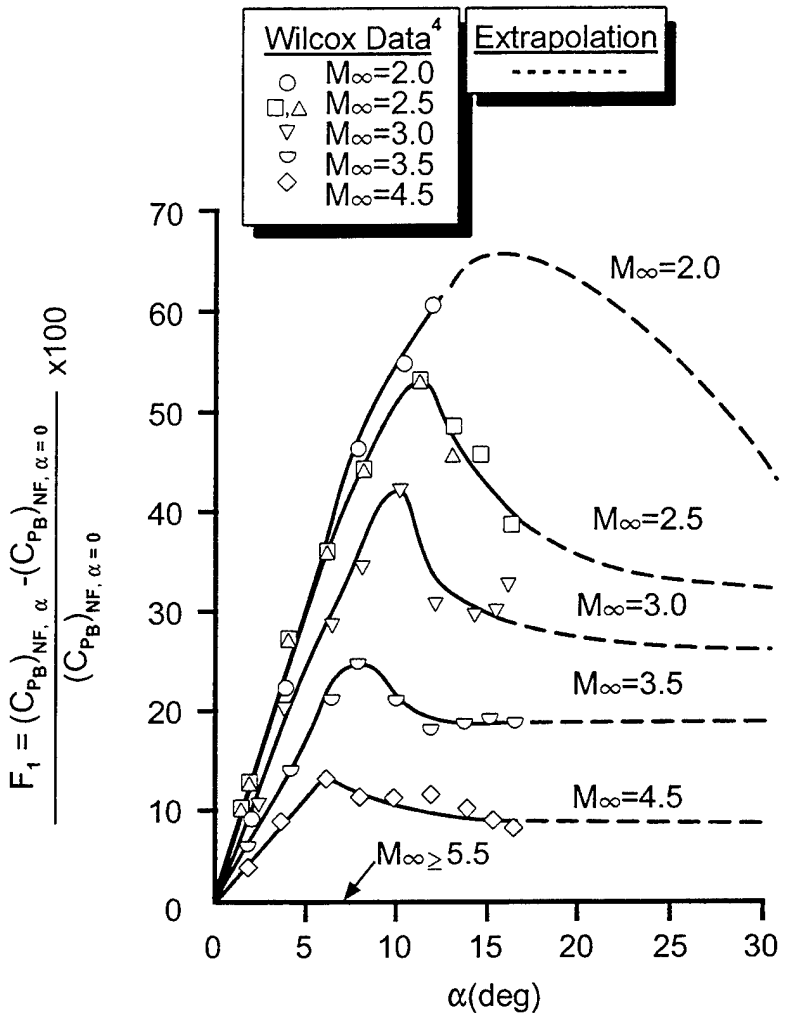

FIGURE 9A. PERCENT INCREASE IN BODY-ALONE BASE PRESSURE COEFFICIENT DUE TO ANGLE OF ATTACK ($M_\infty \geq 2$)

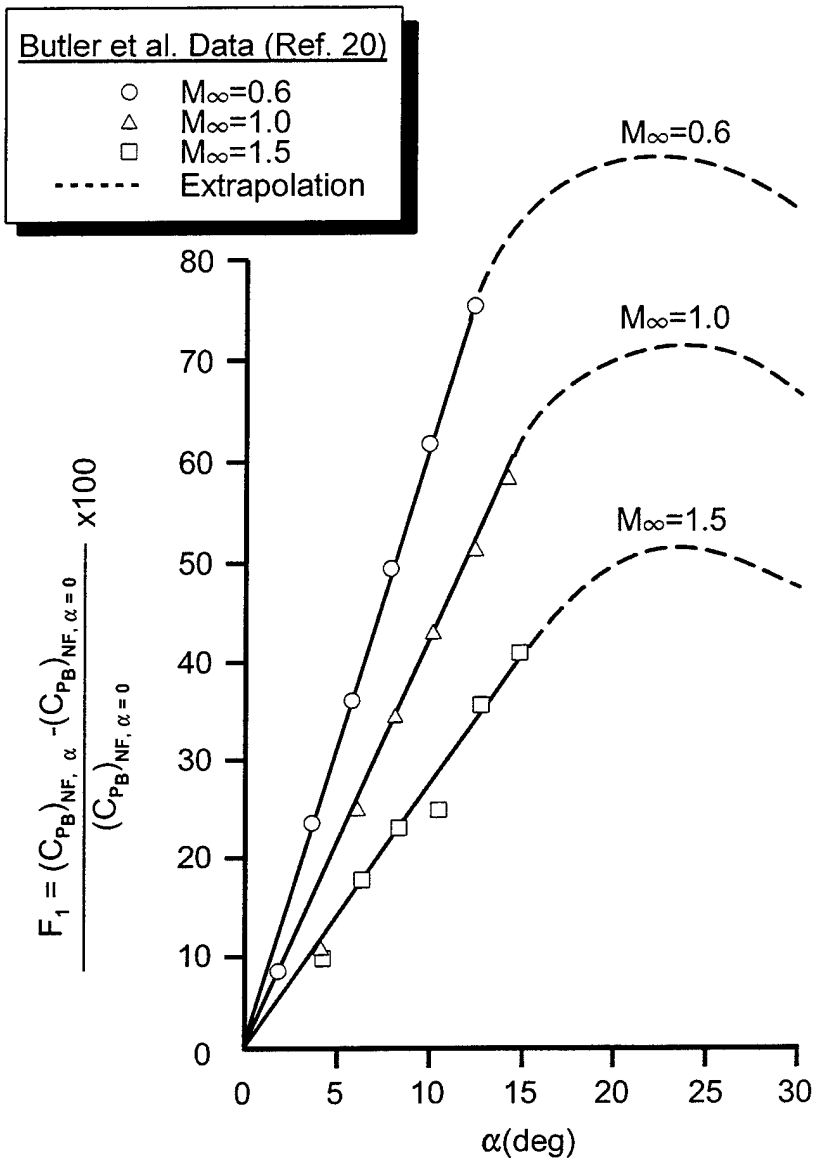

FIGURE 9B. PERCENT INCREASE IN BODY-ALONE BASE PRESSURE COEFFICIENT DUE TO ANGLE OF ATTACK ($M_\infty < 2$)

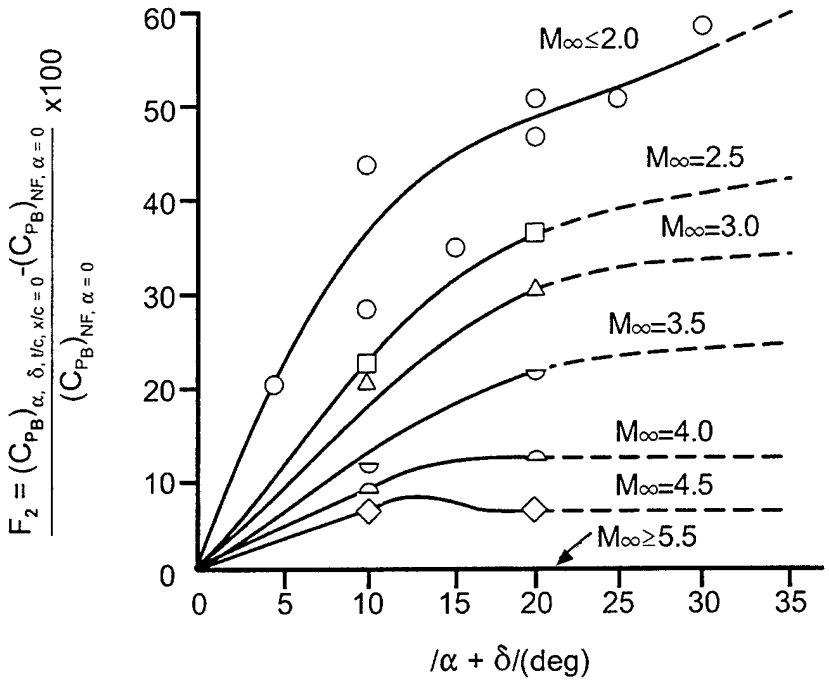

FIGURE 10. PERCENT INCREASE IN BASE PRESSURE COEFFICIENT DUE TO COMBINED EFFECTS OF ANGLE OF ATTACK AND CONTROL DEFLECTION (t/c ≈ 0)

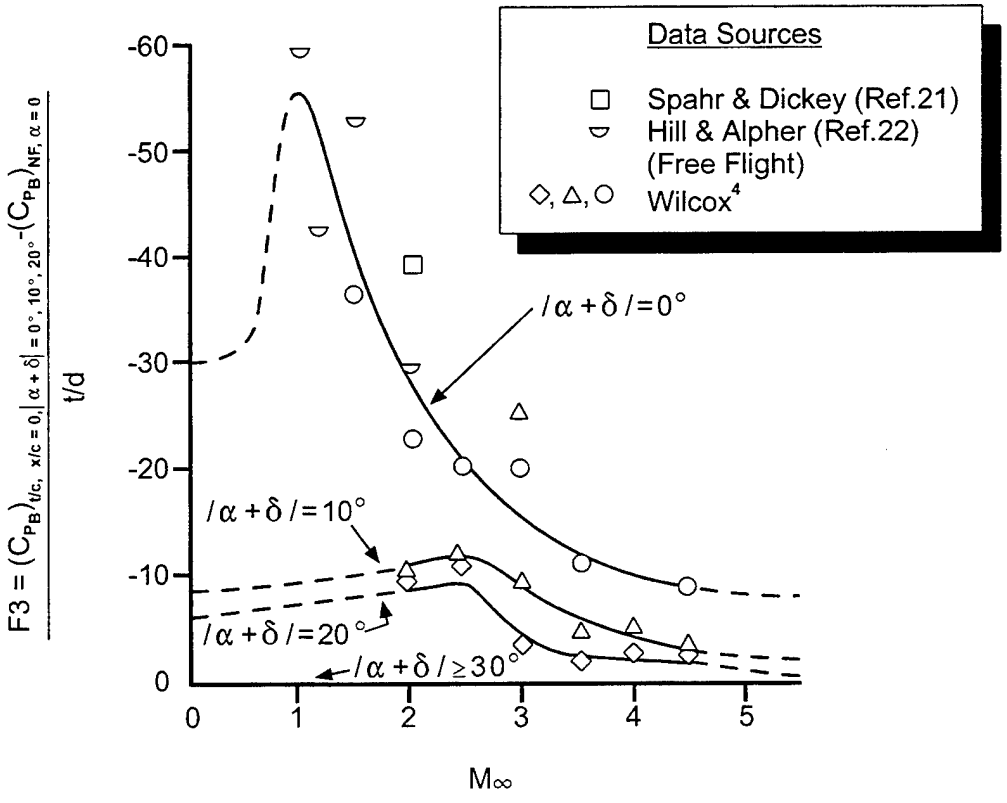

FIGURE 11. PERCENT CHANGE IN BASE PRESSURE COEFFICIENT DUE TO FIN THICKNESS AT VARIOUS VALUES OF $|\alpha + \delta|$

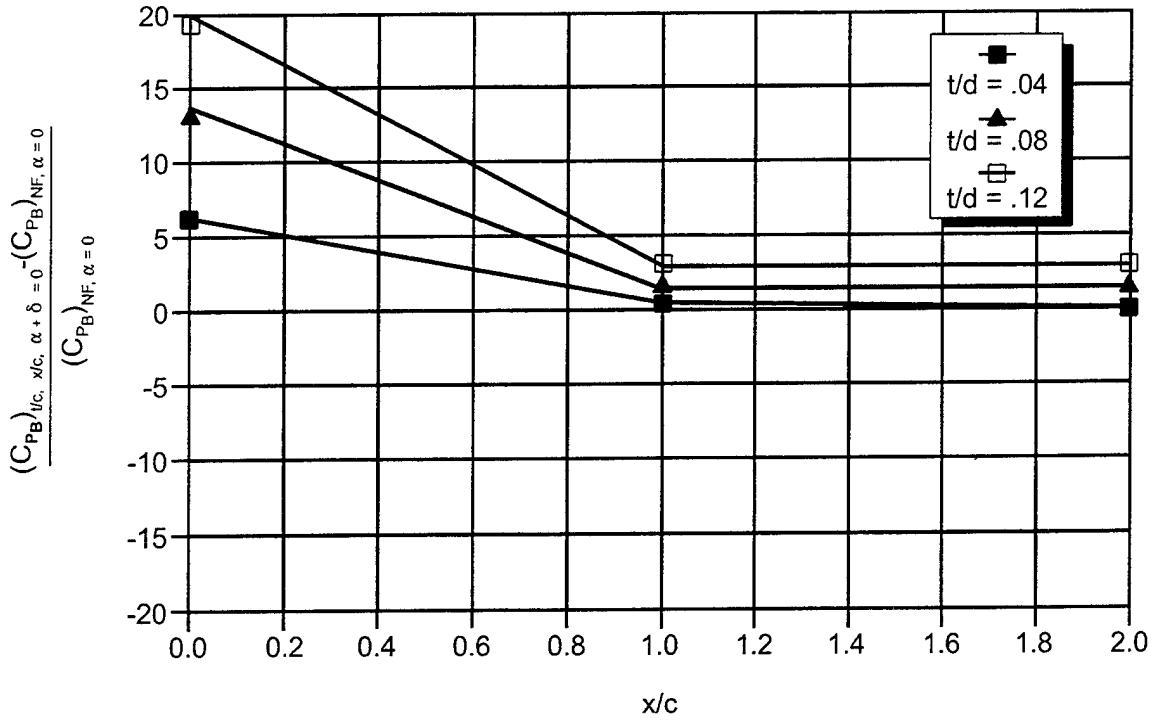

FIGURE 12A. PERCENT INCREASE IN BASE PRESSURE COEFFICIENT DUE TO FIN LOCATION ($|\alpha + \delta| = 0$ DEG, $M_\infty = 2.0$)

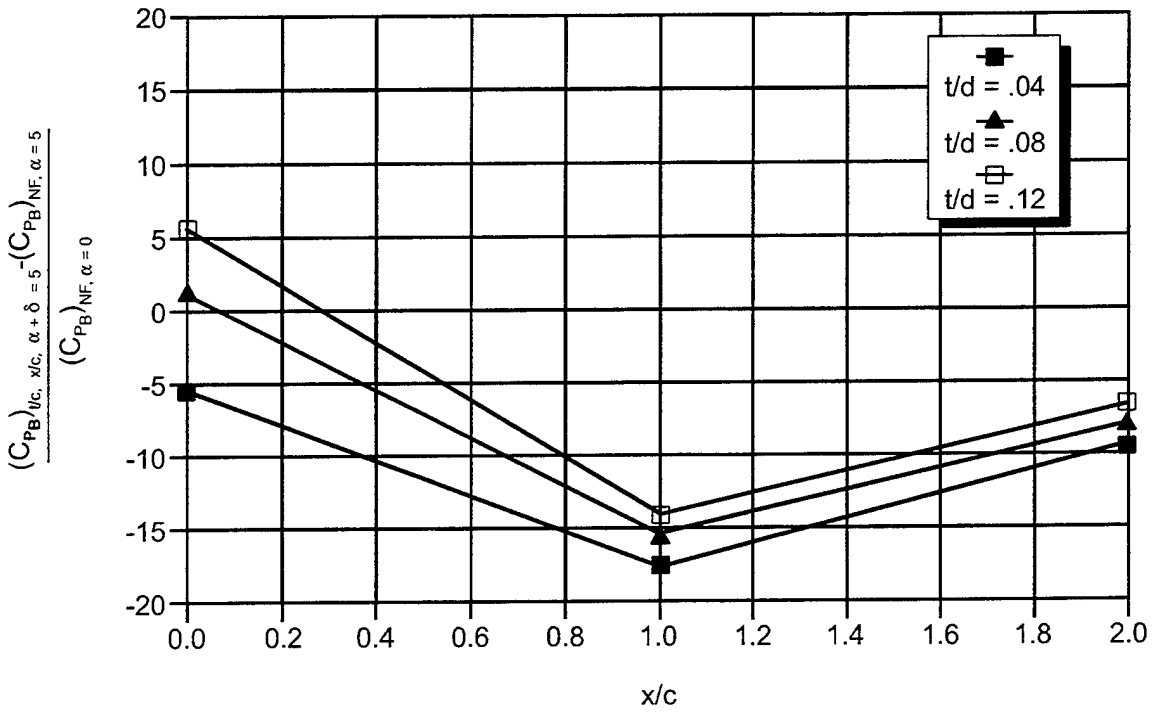

FIGURE 12B. PERCENT INCREASE IN BASE PRESSURE COEFFICIENT DUE TO FIN LOCATION ($|\alpha + \delta| = 5.0$ DEG, $M_\infty = 2.0$)

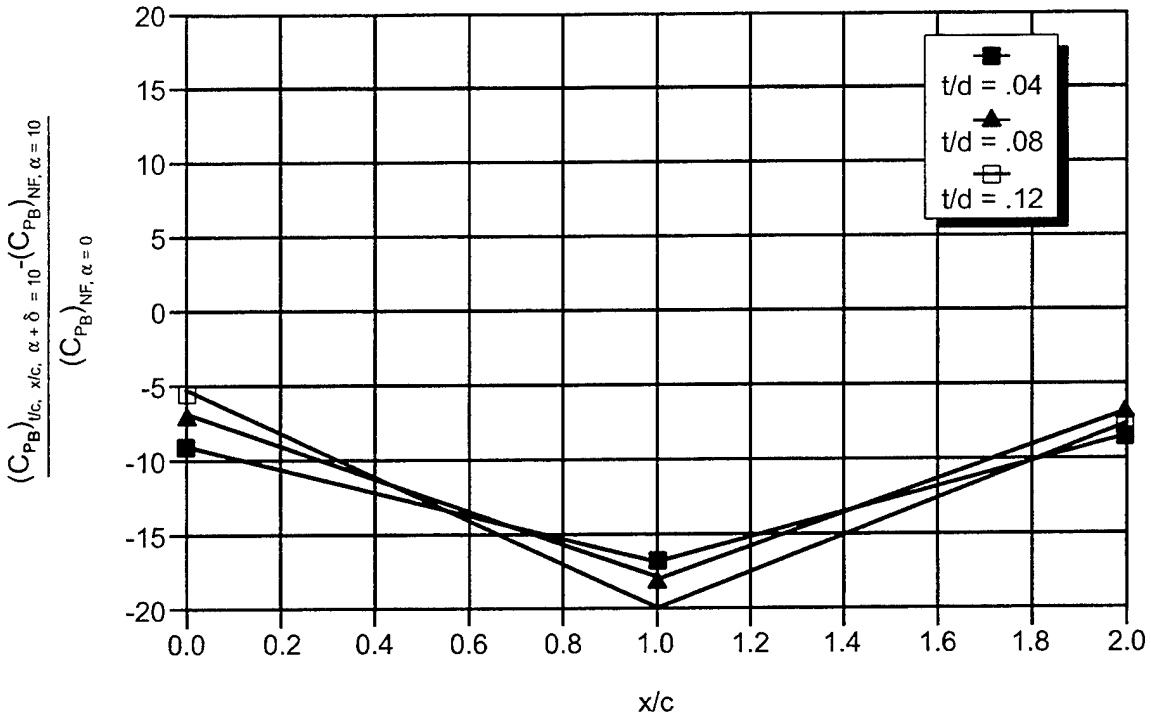

FIGURE 12C. PERCENT INCREASE IN BASE PRESSURE COEFFICIENT DUE TO FIN LOCATION ($|\alpha + \delta| = 10.0$ DEG, $M_\infty = 2.0$)

value of the body alone obtained from Equation (1) of Figure 8. The ΔC_{P_B} term of Equation (3) of Figure 8 is the percent change obtained from interpolation of Figures 12A through 12C. If $|\alpha + \delta| > 10$ deg, Figure 12C is used directly for fin location effects. It is interesting to note that when $|\alpha + \delta| = 0$, Figure 12A shows little effect of fins of reasonable thickness at 1.0 caliber ahead of the base. However, for $|\alpha + \delta| \geq 5$ deg, the fins need to be 2.5 caliber or greater ahead of the base to have negligible effect on base pressure.

Once the final power off value of base pressure coefficient is known from either Equation (1) of Figure 8 (if there are no fins present), or Equations (2) or (3) of Figure 8 (if there are fins present), we now proceed to calculate the change in base pressure coefficient due to power on effects. Since the power-on base drag data was primarily collected for fins off and at zero angle of attack, we will assume the effects of angle of attack and fins will apply to both power-on and power-off conditions. Knowing the value of C_{P_B} with power off or with power on, boattail or flare effects on base pressure are accounted for by Equations (9) or (10), respectively, of Figure 8.

It should be pointed out that the C_{P_B} for the power-on case of Equation (10) in Figure 8 is based on Equations (3) and (4) of Figure 8 because these equations have a term included for boattail or flare. However, the C_{P_B} for the base bleed or power-off conditions of Equation (10)

is based on Table 3, since there is no term to account for the increase in base pressure due to a flare.

TABLE 3. NEGATIVE BASE PRESSURE COEFFICIENTS $\left(-C_{P_B}\right)_f$ FOR VARIOUS FLARE ANGLES AS A FUNCTION OF MACH NUMBER

M_∞	θ_b (deg)			
	0	5	10	≥15
0	0.127	0.170	0.220	0.288
0.2	0.129	0.172	0.222	0.290
0.4	0.131	0.174	0.224	0.292
0.6	0.135	0.176	0.225	0.305
0.8	0.155	0.190	0.237	0.330
0.9	0.195	0.225	0.273	0.367
1.0	0.210	0.250	0.305	0.407
1.1	0.220	0.260	0.305	0.410
1.2	0.225	0.260	0.305	0.405
1.4	0.205	0.235	0.288	0.371
1.6	0.170	0.210	0.239	0.280
2.0	0.145	0.165	0.180	0.192
2.4	0.115	0.133	0.143	0.153
3.0	0.090	0.098	0.104	0.114
3.5	0.070	0.082	0.084	0.086
4.0	0.065	0.065	0.065	0.065
6.0	0.034	0.034	0.034	0.034
10.0	0.029	0.029	0.029	0.029
≥18.4	0.0	0.0	0.0	0.0

Before leaving the empirical model for base drag prediction, some comments are in order. First of all, there are a lot of variables accounted for, and in many cases, the data is limited to definitively account for these variables. It is believed the body alone curve of Figure 7 is quite accurate in predicting power off base drag where the boundary layer ahead of the base is turbulent. It is believed the body alone angle of attack effects for $\alpha \leq 15$ deg of Figure 9 is quite reasonable. However, for $\alpha > 15$ deg, engineering judgement is used in the extrapolation process. It is also believed that the boattail and flare calculations of base axial force of Figure 8 are very accurate. The power on effects of rocket motors and base bleed are reasonable for the conditions assumed. The fin thickness effects of Figure 8 are also reasonable. However, the fin angle of attack effects in conjunction with fin thickness is based on limited data, as are fin location effects. Hence, more engineering judgement is used and it is expected that more errors could occur as well. The final assumption is that the power-on effects are assumed to apply to both configurations with and without fins.

From the previous discussion on assumptions, it is fair to say that more data or computational fluid dynamics computations or both are needed to aid in the definition of base pressure coefficient when several variables are present. This is particularly true for configurations where fins are present and the local angle of attack of the fins is nonzero. However, until more data are available, the empirical model presented here to account for the

various effects on base pressure is believed to be the most comprehensive method available, short of a full Navier Stokes calculation for each case of interest.

3.0 RESULTS AND DISCUSSION

The comparison of the theory and experiment will be separated into the base bleed and power-on base drag predictions. The base bleed results will be discussed first.

3.1 BASE BLEED

There have been several experiments conducted to measure the effect on base pressure of bleeding a small amount of both cold and hot air into the base region of an ogive-cylinder configuration. Figures 5 and 6 illustrate some of these results for cold air conditions with varying Mach numbers and exit area. The modified theory of Danberg will be compared to these and other results for validation.

The first set of results to be considered are those of Bowman and Clayden[10] and Reid and Hastings[9]. They measured base pressure for various Mach numbers with cold air and an exit diameter ratio of $d_j/d_r = 0.4$ (area ratio of 0.16). Figures 13-17 compare the theory to experiment. Figure 13 is for $M_\infty = 1.58$, Figure 14 for $M_\infty = 2.0$, Figure 15 for $M_\infty = 2.5$, Figure 16 for $M_\infty = 3.0$ and Figure 17 for $M_\infty = 3.88$. Figures 13 and 14 show excellent agreement with both the data of Bowman, et al[10] and Reid, et al[9] at $M_\infty = 1.58$ and 2.0, respectively for values of I as high as 0.02. At $M_\infty = 2.5$, (see Figure 15), two sets of data are available. The theory matches the Reference 13 data quite nicely, again to values of $I \cong 0.02$. On the other hand, the data of Bowman, et al[10] appears to be low for both this Mach number and Mach number 3.0 as well. It is suspected that the Reference 10 data is low because of strut interference effects on base pressure for the higher Mach number conditions. Bowman, et al[10] pointed out that their strut was quite thick due to having the air pumped through the strut and into the base region.

The present authors found that with 89 base pressure orifice measurements,[4] fins and struts do indeed affect the base pressure. This effect tends to lower P_B/P_∞ below the value it should be without the interference effect present. We were able to isolate the interference effect to a small region directly behind the fins or strut. When this region was area averaged over the entire base, a lower value of base pressure coefficient was obtained, and a higher value of base drag. With a large number of base pressure taps, the interference effect of the strut would be eliminated. Reference 10 indicated the model diameter was only 1 inch, so it is suspected that not enough pressure taps were available to isolate the interference effect. This effect appears to be the highest at the higher Mach numbers.

Mach 3.0 results are given in Figure 15. Here, the theory is compared to the data of Reference 10 as well as that of Reference 15 for various size exit diameters of the injector. The theory matches the Reference 15 data in an exceptional manner for large values of d_j/d_r (0.67) up

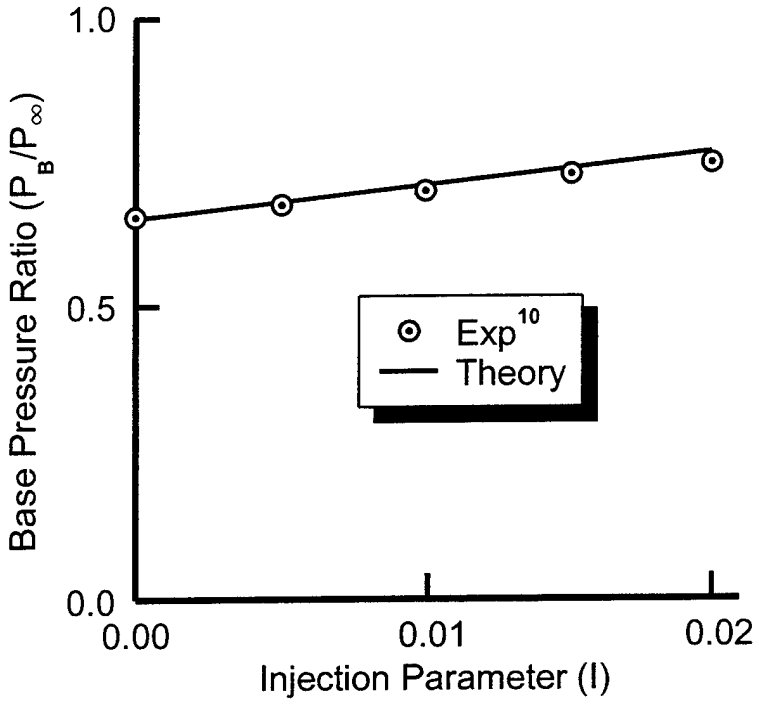

FIGURE 13. COMPARISON OF THEORY AND EXPERIMENT FOR BASE PRESSURE RATIO AT BASE BLEED CONDITIONS (M_∞ = 1.58, dj/dr = 0.4; Tj = 520 °R)

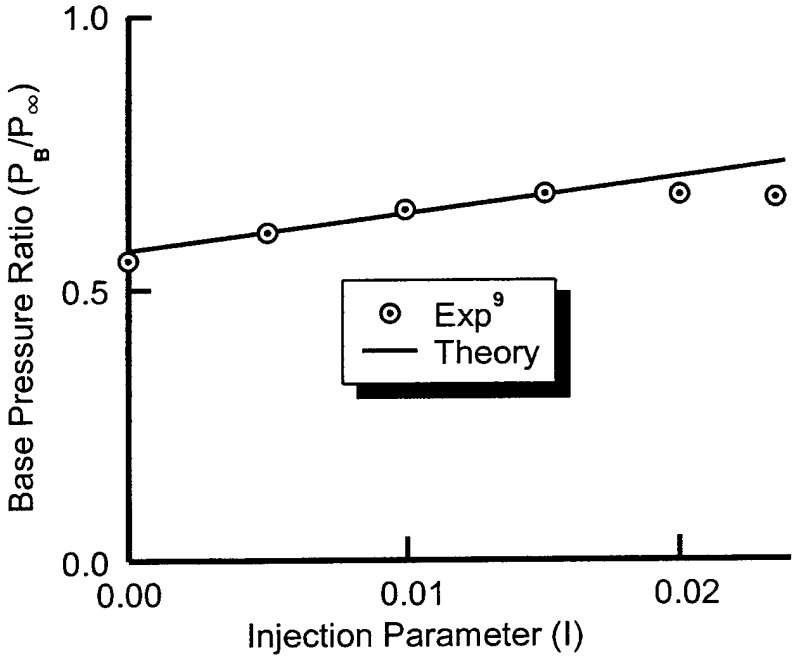

FIGURE 14. COMPARISON OF THEORY AND EXPERIMENT FOR BASE PRESSURE RATIO AT BASE BLEED CONDITIONS (M_∞ = 2.0; dj/dr = 0.4; Tj = 520 °R)

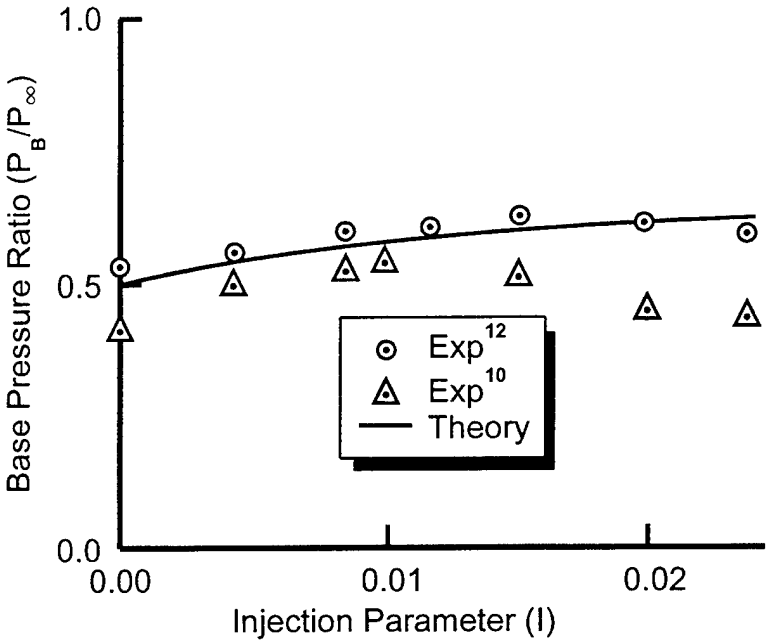

FIGURE 15. COMPARISON OF THEORY AND EXPERIMENT FOR BASE PRESSURE RATIO AT BASE BLEED CONDITIONS (M_∞ = 2.5; dj/dr = 0.4; Tj = 520 °R)

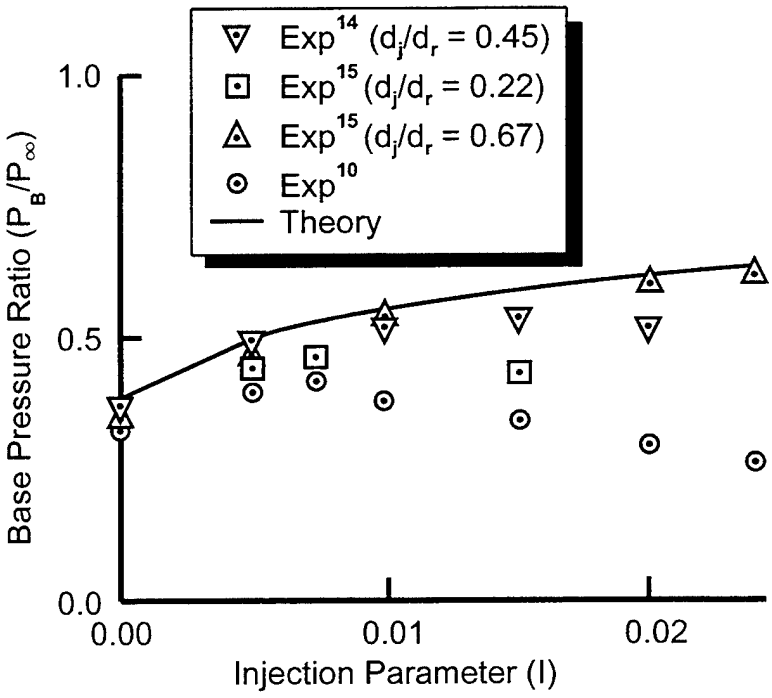

FIGURE 16A. COMPARISON OF THEORY AND EXPERIMENT FOR BASE PRESSURE RATIO AT BASE BLEED CONDITIONS (M_∞ = 3.0; dj/dr = 0.4; Tj = 520 °R)

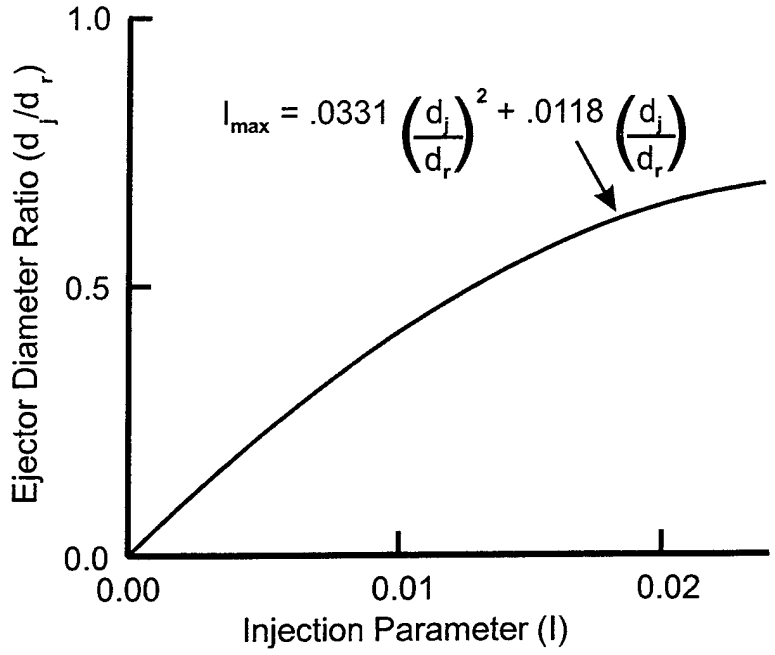

FIGURE 16B. UPPER LIMIT OF I VERSUS dj/dr FOR ACCURATE VALUES OF P_B/P_∞

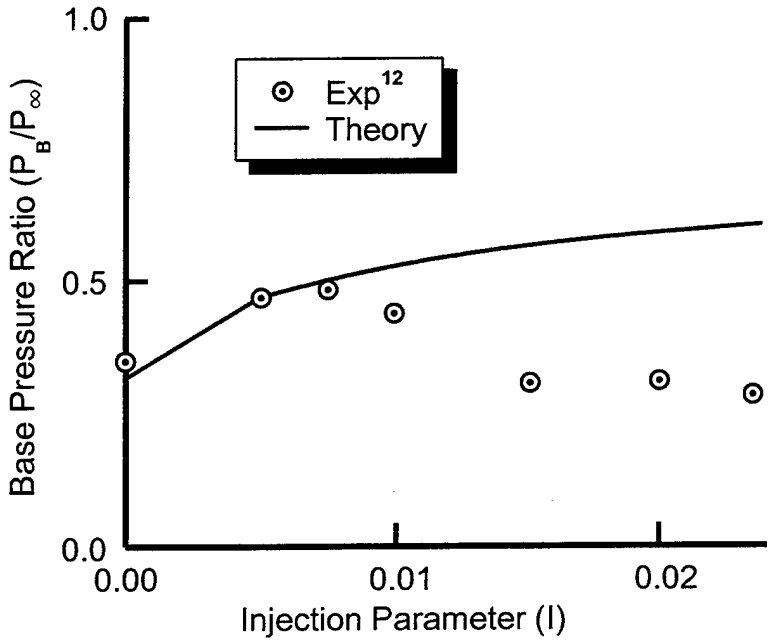

FIGURE 17. COMPARISON OF THEORY AND EXPERIMENT FOR BASE PRESSURE RATIO AT BASE BLEED CONDITIONS (M_∞ = 3.88; dj/dr = 0.4; Tj = 520 °R)

to values of I of 0.025. However, for the smaller values of d_j/d_r of 0.22, theoretical computations are reasonable for I of 0.005 and less. However, for $d_j/d_r = 0.45$, the theory can be used up to values of I of 0.01. An empirical constraint, which can be used as an application guideline for the modified theory of Danberg, is shown in Figure 16B based on the results of Figure 16A. The equation shown in the figure,

$$I_{max} = 0.0331\left(\frac{d_j}{d_r}\right)^2 + 0.0118\left(\frac{d_j}{d_r}\right) \tag{23}$$

gives the maximum value of I for a given value of ejector diameter ratio where accurate values of P_B/P_∞ can be expected from the theory. This equation is expected to be conservative for Mach numbers less than 3.0 and may be optimistic for Mach numbers greater than 3.0. This statement is based on the fact that as Mach number decreases, the value of I where accurate results of P_B/P_∞ can be expected increases for a fixed value of $d_j/d_r = 0.4$.

The last comparison of predicted base pressure with Mach number at room temperature conditions is shown on Figure 17 for $M_\infty = 3.88$. The experimental data is taken from Reference 12. As seen in the figure, acceptable accuracy can be obtained for values of I up to about 0.008.

Several cases were found where hot gas was used as the injectant. The first of these cases is taken from Reference 23 and comparisons of theory and experiment at $M_\infty = 0.71$ and 0.98 are shown in Figures 18 and 19, respectively. Temperature of the gas is 2150 °R and the ejector diameter ratio is 0.31. Comparison of theory to experiment is excellent for both Mach numbers, although data was only available for values of $I \leq 0.008$.

The next hot gas data is taken from Reference 11. Bowman and Clayden[11] used argon heated to a range that varied from room temperature (520 °R) to 9126 °R at $M_\infty = 2.0$. The modified theory is compared to the Reference 11 data for a T_j value for 5400 °R where $d_j/d_r = 0.2$ in Figure 20. Recall from Figure 16 that for values of $d_j/d_r = 0.2$, the maximum value of I where accurate results of the theory can be expected for a cold gas is approximately 0.0037. As seen in Figure 20, for a hot gas, this value of .0037 is too high by about a third. In other words, for a hot gas, the limiting values computed for I_{max} by Equation 23 should be reduced somewhat. However, since the maximum value of base pressure ratio occurs at approximately 0.0008 to 0.0022 for this case, the theory is still reasonable for the practical case. That is because one would choose a value of I in the design process to give maximum values of P_B/P_∞. Also, for a hot gas, Equation 23 should be modified according to

$$(I_{max})_{hot} \cong \frac{2}{3}[I_{max}]_{cold} \tag{24}$$

Figure 21 summarizes the revised mathematical model of Danberg that will be incorporated into the AP02. The revisions specifically included in the Danberg model are use of the AP02 empirical data base to predict $(P_B/P_\infty)_{I=0}$; using a constant value for β of 2.6 versus

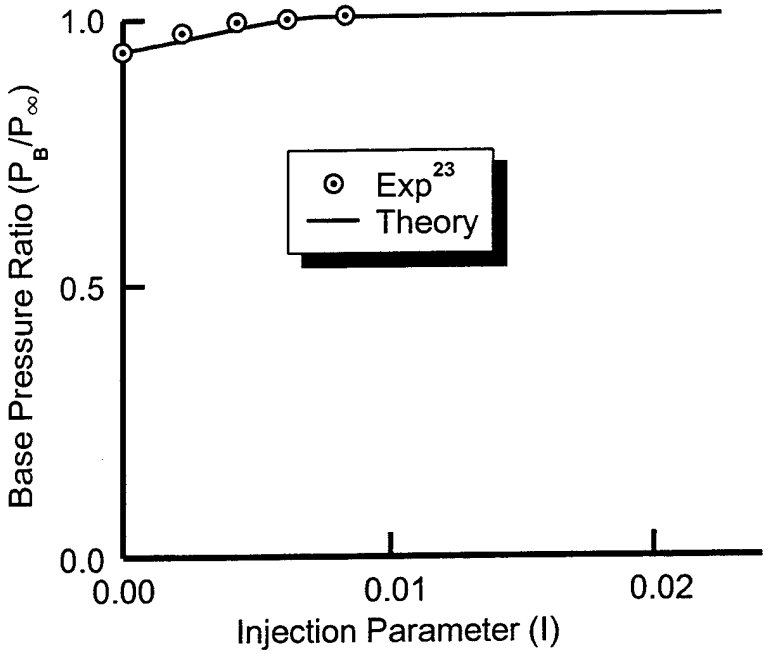

FIGURE 18. COMPARISON OF THEORY AND EXPERIMENT FOR BASE PRESSURE RATIO AT BASE BLEED CONDITIONS (M_∞ = 0.71; dj/dr = 0.31; Tj = 2150 °R)

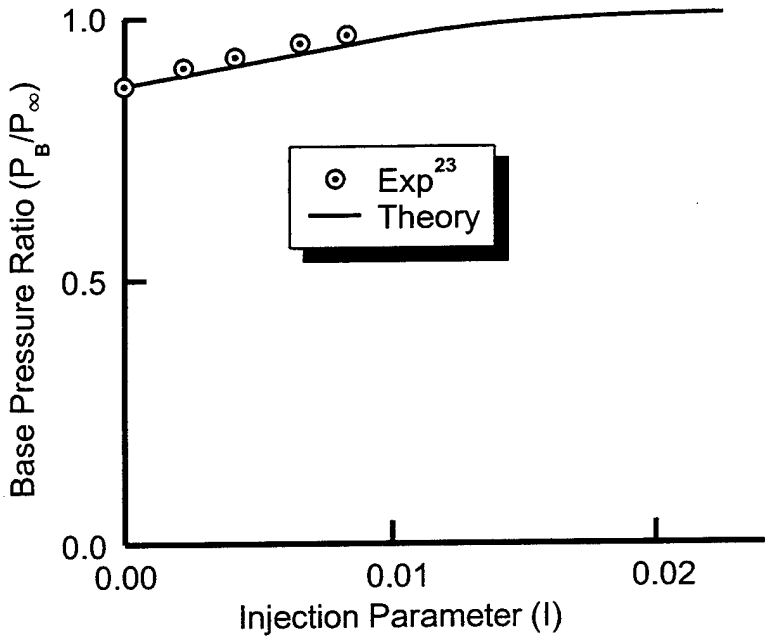

FIGURE 19. COMPARISON OF THEORY AND EXPERIMENT FOR BASE PRESSURE RATIO AT BASE BLEED CONDITIONS (M_∞ = 0.98; dj/dr = 0.31; Tj = 2150 °R)

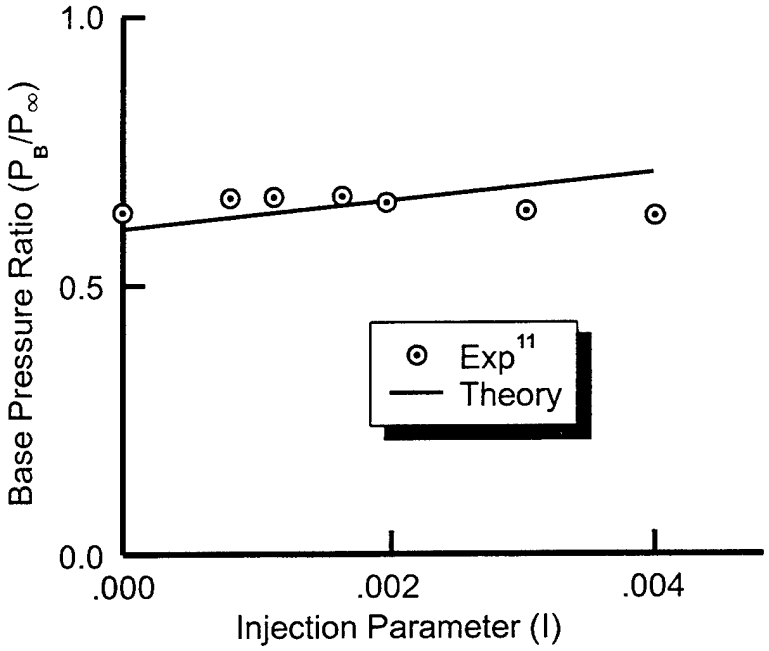

FIGURE 20. COMPARISON OF THEORY AND EXPERIMENT FOR BASE PRESSURE RATIO AT BASE BLEED CONDITIONS (M_∞ = 2.0; dj/dr = 0.2; Tj = 5400 °R)

Equation (20b); and defining a range of values of I as a function of exit diameter ratio that accurate values of P_B/P_∞ can be expected from the theory.

The 155 mm M864 projectile of Reference 3 (see Figure 22A) is used here as a practical illustration example of the modified base bleed theory of Danberg, which will be incorporated into the aeroprediction code and be transitioned as the AP02. The M864 configuration is 5.79 calibers in length with a 3.42 caliber truncated nose. The boattail is 0.5 caliber and has a 3 deg boattail angle. Figure 22B compares the AP02 predictions of zero lift drag to the ballistic range and NS computations taken from Reference 3. In general, the AP02 gives quite acceptable agreement to the experimental data, and in most cases is slightly better than the NS calculations. Figure 22C compares the AP02 zero lift drag calculations for values of I = 0, 0.0025 and 0.005. These values of I cover the practical range of interest. Notice the drag reduction effect of base bleed. The effect is particularly pronounced at Mach numbers less than about 0.9. For illustration purposes, the M864 boattail length was increased from 0.5 to 1.0 caliber and the angle increased from 3 to 7 deg. Values of C_{D_0} for this case are shown with the open symbol in Figure 22C. Note that the drag reduction is about comparable to the base bleed parameter value I = 0.0025 for $M_\infty \geq 0.7$. The point of illustration is to show why base bleed is used in design tradeoffs and for specific applications, but is not the author's preferred choice for range increase. The reasons are several fold. First, the drag reduction from a boattail occurs in a passive manner throughout the flight of a projectile and is repeatable with fairly low ballistic errors. It also is low cost. Base bleed, on the other hand, has additional costs, and for practical values of I, is no better in drag reduction than a good boattail design.

$$\frac{P_B}{P_\infty} = \left(\frac{P_B}{P_\infty}\right)_{I=0} + \frac{\sigma I}{1 + 2.6\sigma I}$$

where:

$\left(\frac{P_B}{P_\infty}\right)_{I=0}$ from AP02 Empirical Data Base

$$\sigma = \left(-5.395 + 0.0172T_j\right)M_\infty + \left(4.61 - 0.0146T_j\right)M_\infty^2$$
$$+ \left[-0.566 + 0.00446T_j\right]M_\infty^3$$

I = Injection Parameter

T_j = Exit Temperature (deg Rankine)

$$I_{max} = (0.0331)\left(\frac{d_j}{d_r}\right)^2 + (0.0118)\left(\frac{d_j}{d_r}\right) \text{ for cold gas}$$

$$(I_{max})_{Hot\ gas} = 2/3\left[I_{max}\right]_{Cold\ gas}$$

I_{max} = Maximum value of I for given value of d_j/d_r where accurate values of P_B/P_∞ can be expected

FIGURE 21. REVISED DANBERG[3] MODEL FOR BASE BLEED

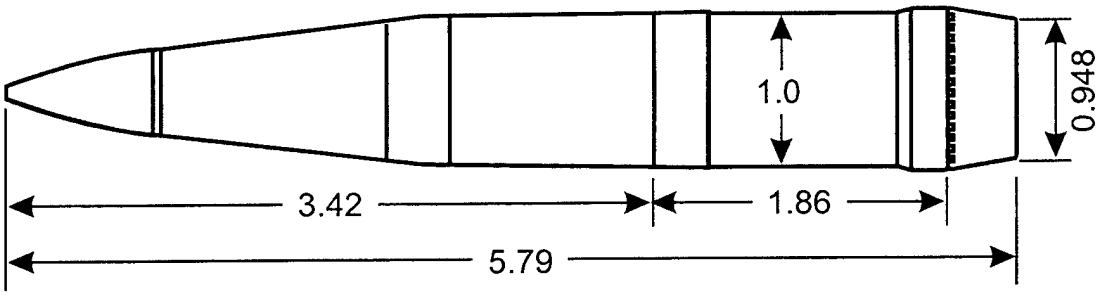

FIGURE 22A. M864 155 MM PROJECTILE (ALL DIMENSIONS IN CALIBERS)

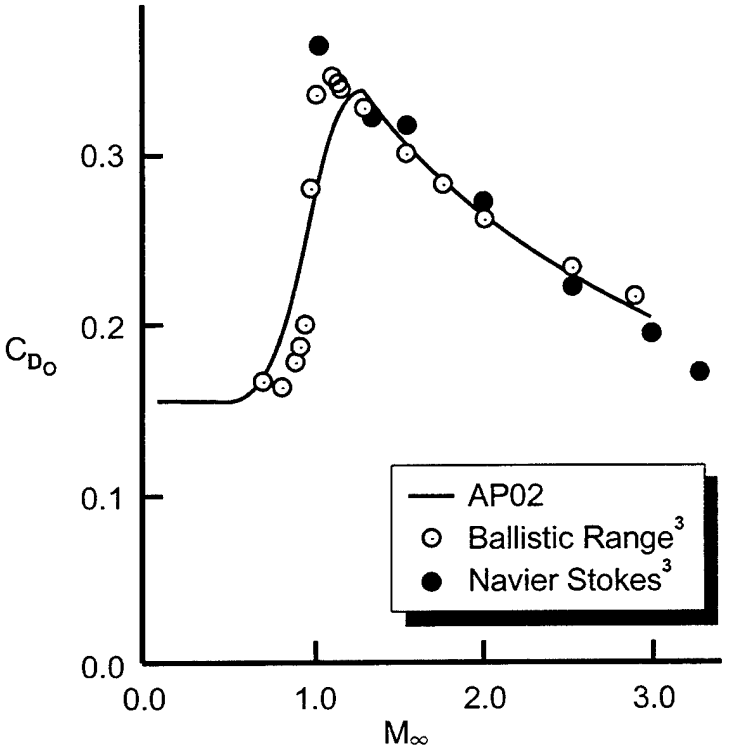

FIGURE 22B. ZERO LIFT DRAG COMPARISONS OF THEORY AND EXPERIMENT FOR 155 MM, M864 PROJECTILE (I = 0)

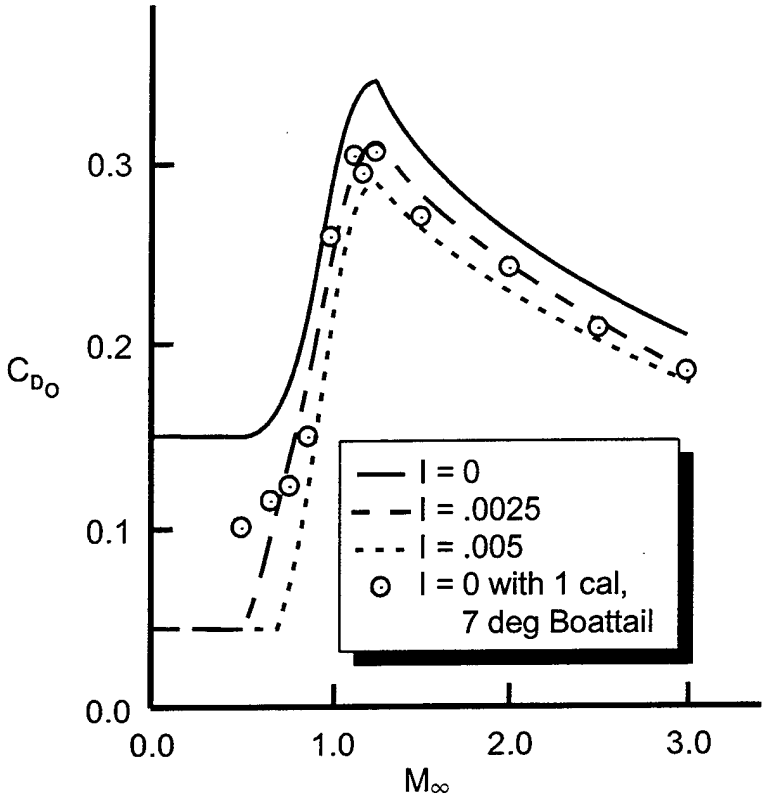

FIGURE 22C. ZERO LIFT DRAG OF M864 PROJECTILE FOR TYPICAL VALUES OF BASE BLEED

A second practical example is taken from Reference 24 where NS calculations were performed on a cylindrical based afterbody at $M_\infty = 1.7$ and 2.5 for values of the mass injection parameter of 0 to 0.03. These NS results were then compared in Reference 24 to the experimental data of Schilling[25]. The AP02 computations for this same case at $M_\infty = 1.7$ and 2.5 are compared to both the experimental results of Schilling[25] and CFD results of Sahu[24] in Figure 23. At $M_\infty = 1.7$, the AP98 result for C_{A_B} at I = 0 is slightly higher than either the Reference 24 or 25 results. The decrease in C_{A_B} with increasing I is parallel to the experiment and CFD up to values of I of about 0.02 to 0.025 for this room temperature case. At $M_\infty = 2.5$, the AP02 agrees very well with the experimental data[25] and CFD[24] predictions up to values of I = 0.012 before the AP02 results depart from the more accurate theory or experimental results. Again, since the practical range of interest for I is generally 0.01 or less, this level of agreement with the data is viewed as being acceptable.

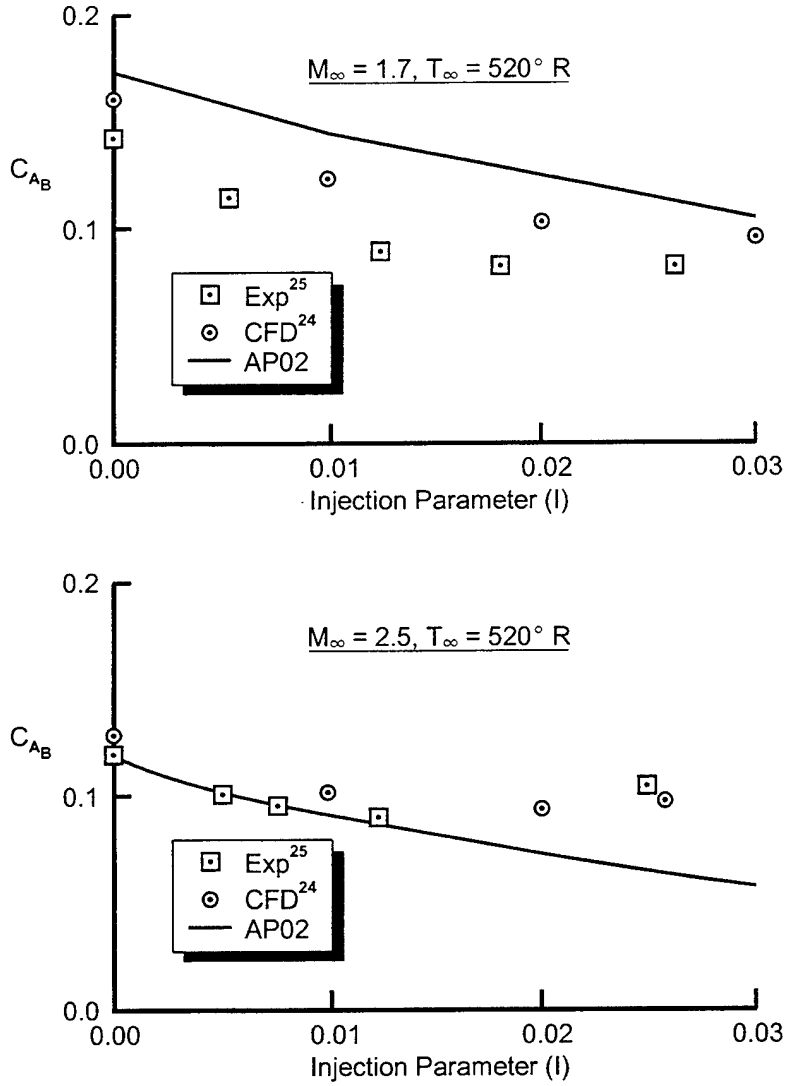

FIGURE 23. COMPARISON OF THEORY AND EXPERIMENT FOR BASE DRAG AS A FUNCTION OF MASS INJECTION PARAMETER

3.2 POWER ON BASE DRAG FOR ROCKETS

The first case to compare the present predictions of power on base pressure are results taken from Reference 9 and correlated by Brazzel as a function of the Jet Momentum Flux parameter RMF. These results, shown in Figure 24, were for various jet to reference diameter ratios at $M_\infty = M_j = 2.0$. Also shown in Figure 24 are the predictions of the Brazzel method (indicated by the AP98) for the low values of RMF computed from Equation (1) for various values of RMF assuming $\gamma_j = 1.4$ and $x_j = 0$. Since $M_j = 2$, $T_j / T_j^* = 0.67$ for Figure 24. Also shown on Figure 24 are the results for the improved method to be incorporated into the AP02 (see Equation 11). As seen in Figure 24, both the Brazzel technique and the AP02 method predict base pressure slightly high compared to the Reference 9 data. This means base drag would be slightly low compared to the Reference 9 experimental data.

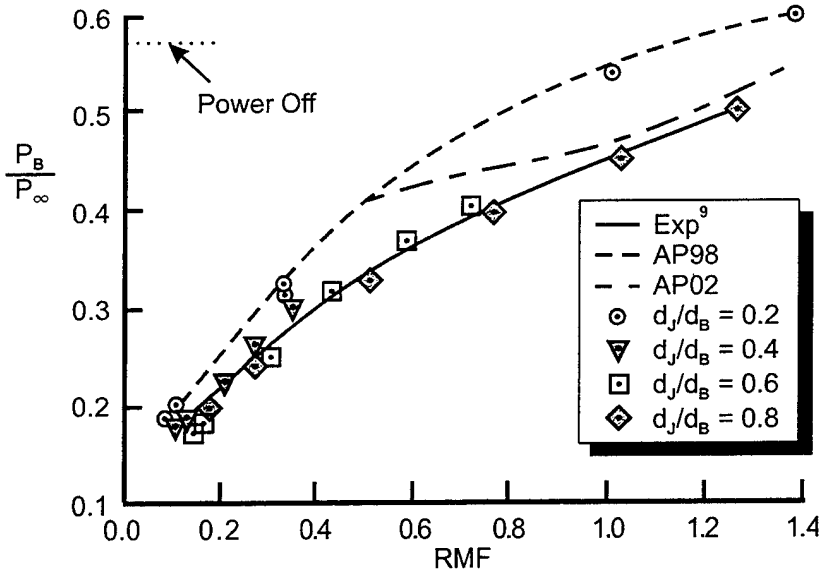

FIGURE 24. COMPARISON OF POWER-ON-BASE PRESSURE PREDICTION WITH EXPERIMENT (Mj = 2.0, M_∞ = 2.0)

The second case considered is taken from the data of Bromm, et al[26] for a cylindrical afterbody configuration. The data is for sonic jet exit conditions at M_∞ = 2.41 and d_j/d_B = 0.5. Figure 25 compares the theory of AP02 to the experiment. Theoretical predictions give quite satisfactory comparisons to data with the base drag being somewhat high compared to data. The theory here is basically that of Brazzel, et al[1] up to P_j/P_∞ of about 10. Above P_j/P_∞ of 30, there is a slight improvement of the AP02 over the AP98 prediction. However, the AP02 gives slightly worse comparisons to experiment than the AP98 for values of P_j/P_∞ between 10 and 30. Both the AP98 and AP02 agreement with experiment is considered acceptable, as either would give only small errors in axial force coefficient.

The next case considered is taken from the data of Reference 5. M_∞ = 1.5 and 2.5 cases are shown for the M_j = 1.0, and d_j/d_r = 0.45 conditions in Figure 26. The AP02 gives excellent comparison to experiment at M_∞ = 2.5 and reasonable agreement at M_∞ = 1.5. The power off base pressure coefficient is noted for both the M_∞ = 1.5 case $\left(C_{P_B} = -0.19\right)$ and M_∞ = 2.5 case $\left(C_{P_B} = -0.115\right)$. This figure illustrates how power-on can actually increase base drag over no power-on at some conditions, while at other conditions, base drag can be changed to base thrust.

The next case considered is taken from Reference 27 and is for M_j = 2.5, M_∞ = 1.94 and d_j/d_r = 0.75. In addition to the experimental data of Reference 27, the data of Reference 6 is also shown in Figure 27. The AP02 compares fairly well with the Reference 6 data at lower values of C_T and is in between the Reference 6 and Reference 27 data for higher values of C_T. Once again, the power-off base pressure coefficient is shown on the Figure 27, illustrating that at very low values of thrust coefficient, power on increases base drag, whereas for higher values of C_T, base drag is decreased.

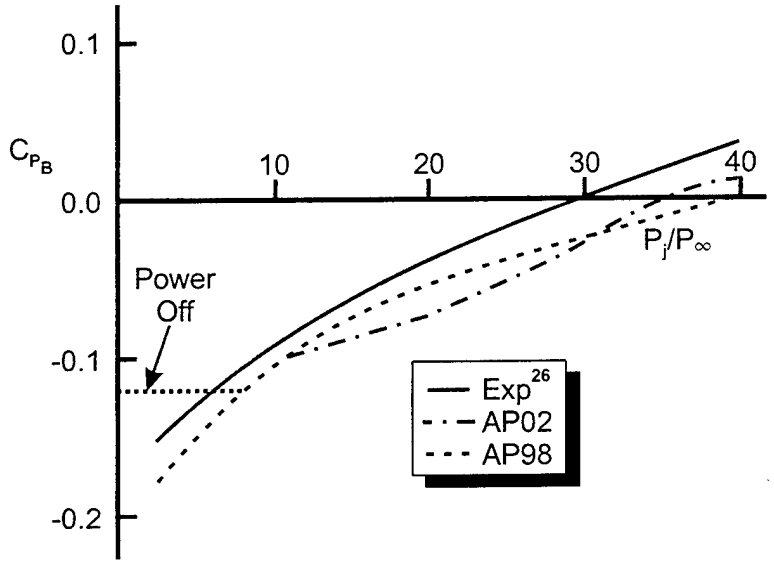

FIGURE 25. COMPARISON OF POWER-ON-BASE PRESSURE COEFFICIENT PREDICTION WITH EXPERIMENT (Mj = 1, M_∞ = 2.41, dj/d_B = 0.5)

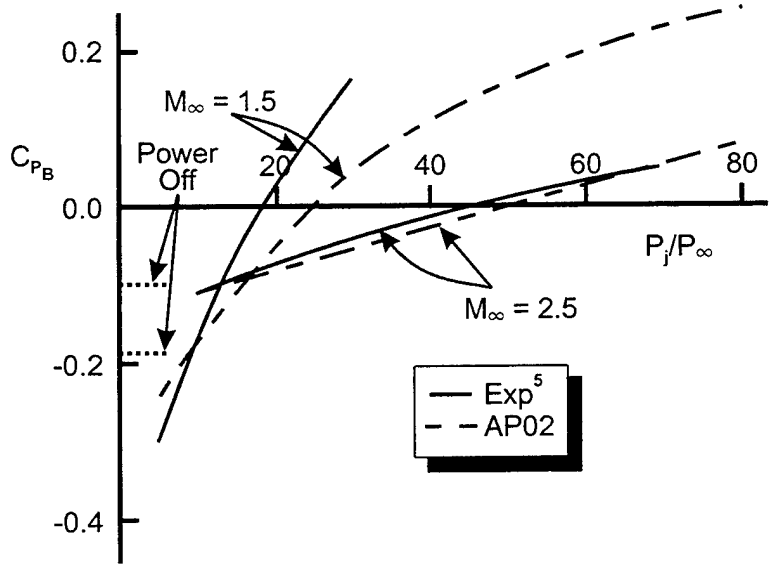

FIGURE 26. COMPARISON OF POWER-ON-BASE PRESSURE COEFFICIENT PREDICTION WITH EXPERIMENT (Mj = 1.0, dj/d_B = 0.45)

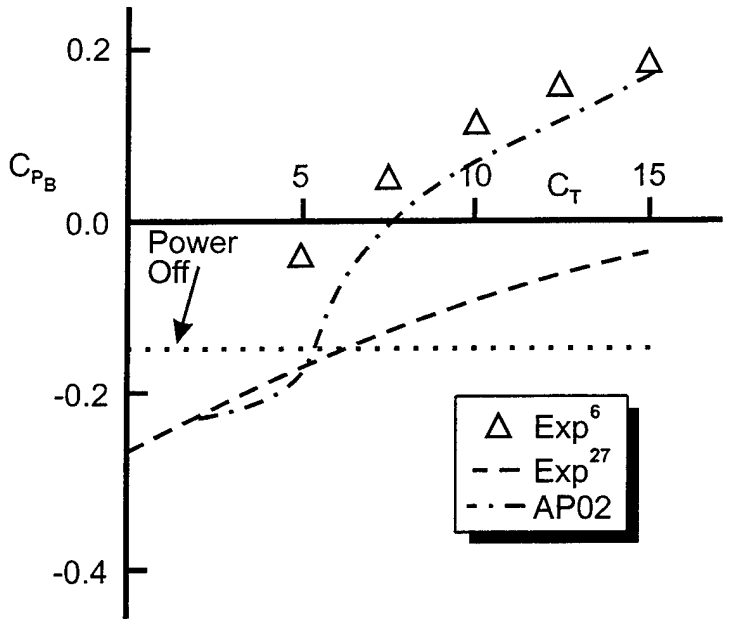

FIGURE 27. COMPARISON OF POWER-ON-BASE PRESSURE COEFFICIENT PREDICTION WITH EXPERIMENT (Mj = 2.5, M_∞ = 1.94, dj/dr = 0.75)

Figure 28 illustrates results for jet exit Mach number of 3.5, where the other conditions (M_∞ = 1.94, d_j/d_r = 0.75) are the same as those in Figure 27. Again, the AP02 is in agreement with the Reference 6 data at low values of C_T and is in between the Reference 27 and Reference 6 data for high values of C_T.

Figure 29 compares the AP02 predictions for C_{P_B} to the data from Reference 26 for two sets of exit Mach numbers (M_j = 1.78 and M_j = 2.7) for M_∞ = 2.5 and d_j/d_r = 0.2. Results are shown for fairly low values of thrust coefficient. Reasonable agreement is obtained for both cases, with errors in C_{P_B} predictions of up to 20 percent. Errors in C_{A_B} and C_A will be reduced considerably due to the fact C_{P_B} only acts over the area outside the exit and C_{A_B} is only a portion of the total axial force.

Petrie, et al[28] conducted experiments to measure power on base pressure on a tangent ogive cylinder with freestream Mach number of 1.4, and jet exit Mach number of 2.2. Two pressure ratios at the exit were considered, P_j/P_∞ = 2.15 and 6.44. Petrie invited outside participants to perform both semiempirical predictions as well as various NS calculations to predict base pressure at these two conditions. For P_j/P_∞ = 2.15 and RMF = 0.32, the present method is that of Brazzel so that P_b/P_∞ = 0.25 based on Equation (10). This compares to an average experimental value of P_b/P_∞ = 0.4, or an error of 37.5 percent. The other semiempirical models gave somewhat better predictions as the errors varied from about 12 percent too high to 20 percent too low. However, NS predictions gave errors that were 35 to 50 percent too high. For the P_j/P_∞ = 6.44 case, RMF= 0.96. Here, Equation (10) yields slightly different results from that of Brazzel as P_b/P_∞ = 0.34. This compares to an average experimental value of P_b/P_∞ = 0.44,

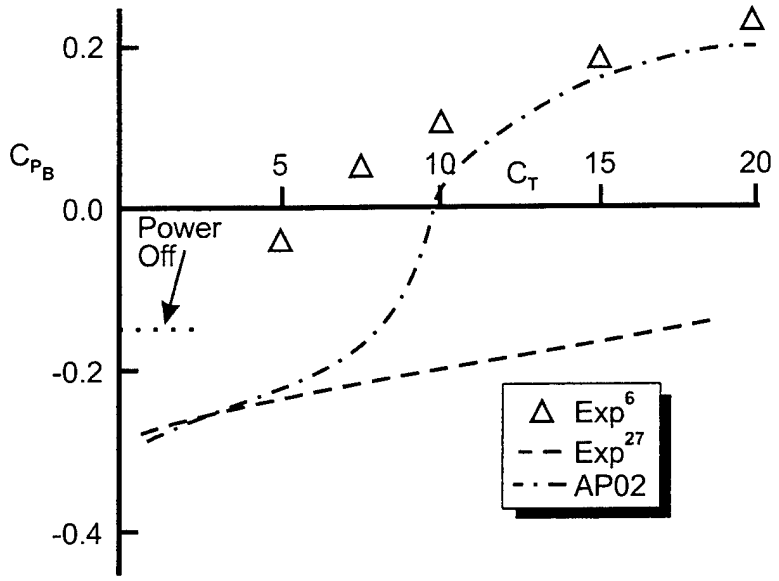

FIGURE 28. COMPARISON OF POWER-ON-BASE PRESSURE COEFFICIENT PREDICTION WITH EXPERIMENT (Mj = 3.5, M_∞ = 1.94, dj/d_B = 0.75)

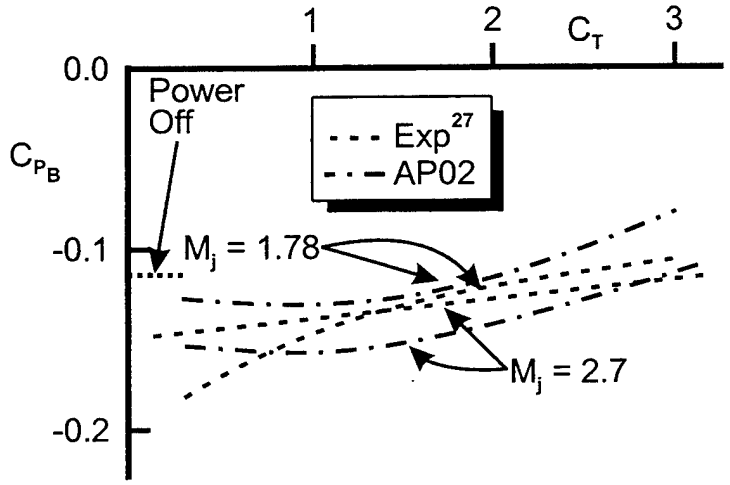

FIGURE 29. COMPARISON OF POWER-ON-BASE PRESSURE COEFFICIENT PREDICTION WITH EXPERIMENT (M_∞ = 2.5, dj/dr = 0.2)

giving an error of about 23 percent. For this case, the present predictions are better than the semiempirical prediction errors presented in Reference 28 (35 percent) or the NS predictions (32 percent). This example illustrates the difficulty in accurately predicting base pressure coefficient and also the wide spread in prediction values from the various theoretical methods available.

The next three examples are taken from the experimental database of Rubin.[29] Rubin measured power on base drag in the transonic speed regime for cylindrical, flare, and boattail afterbodies at transonic Mach numbers. Figure 30 compares the semiempirical predictions to the data of Rubin for the cylindrical afterbody at M_∞ = 0.9, 1.0, and 1.2. Experimental data was based on M_j = 2.7 and d_j/d_B = 0.8 and 0.45. A conical nozzle was used with θ_j = 20 deg. The agreement between the experiment and theory at all three Mach numbers is reasonable. However, for M_∞ = 0.9 and $C_T < 4$, the experimental data shows P_b/P_∞ increasing. The present theory will not predict the minimum base pressure ratio. This increase in P_B/P_∞ will continue as C_T gets small until a maximum is reached at base bleed conditions, after which P_B/P_∞ will decrease to its power-off value.

Figure 31 presents the comparison of theory and experiment for the boattailed afterbody case. Results for the same three freestream Mach numbers (M_∞ = 0.9, 1.0, and 1.2) are shown on the figure. The boattail angle is 6.35 deg and the boattail length is 0.82 caliber. Again, reasonable agreement with experiment is seen except for M_∞ = 0.9 and 1.0 and for low values of C_T, where the minimum value of P_B/P_∞ has been reached.

Figure 32 presents the comparison of theory and experiment for the flare afterbody case. The flare angle is 6.54 deg and its length is 1.34 caliber. Good agreement between theory and experiment is seen, except for M_∞ = 0.9 and $C_T < 6$, where the base pressure is seen to start increasing after a minimum has been reached.

The last case considered is a boattailed configuration taken from the data of Craft and Brazzel.[5] Theory and experiment are shown in Figure 33 for M_∞ = 1.5 and 2.5. Again M_j = 2.7, d_j/d_r = 0.45, θ_j = 20 deg, θ_B = 2.93 deg and ℓ_B = 1.37 calibers. Very good agreement of theory and experiment is obtained at M_∞ = 1.5. However, for M_∞ = 2.5 the theory is about 10 to 30 percent too high for $C_T \geq 8$. The reason for the overprediction is not clear. However, it is to be suspected that the error is due to the Reference 6 data base being given more weight in the development of the present empirical model than the Reference 5 data base. As seen in Figure 3B, the Reference 6 data is higher than the Reference 5 data. The discrepancy is unclear. One author of another reference did indicate that he had to ignore his M_∞ = 2.0 data due to the fact the bow shock wave reflected from the wind tunnel wall into the base flow area, causing erroneous readings at this condition.

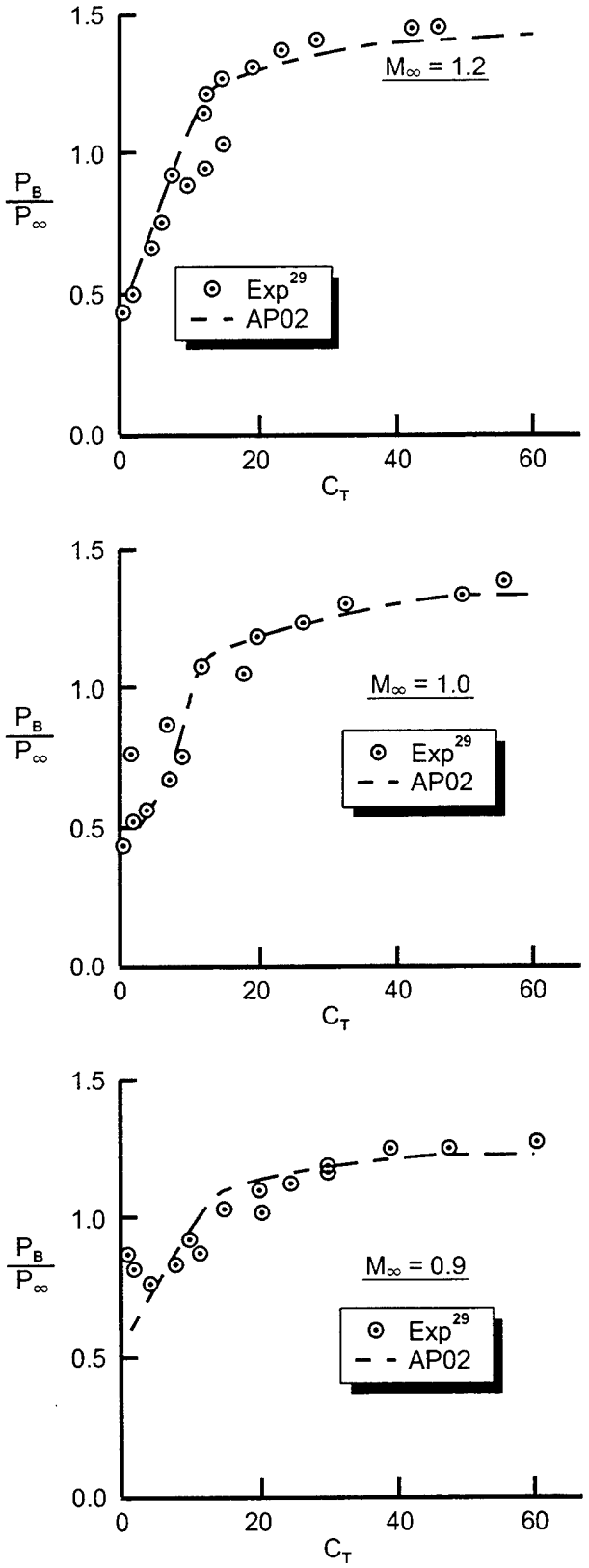

FIGURE 30. COMPARISON OF POWER-ON-BASE PRESSURE PREDICTION WITH EXPERIMENT FOR CYLINDRICAL AFTERBODY (Mj = 2.7; dj/d_B = 0.8, 0.45; θ_j = 20 DEG)

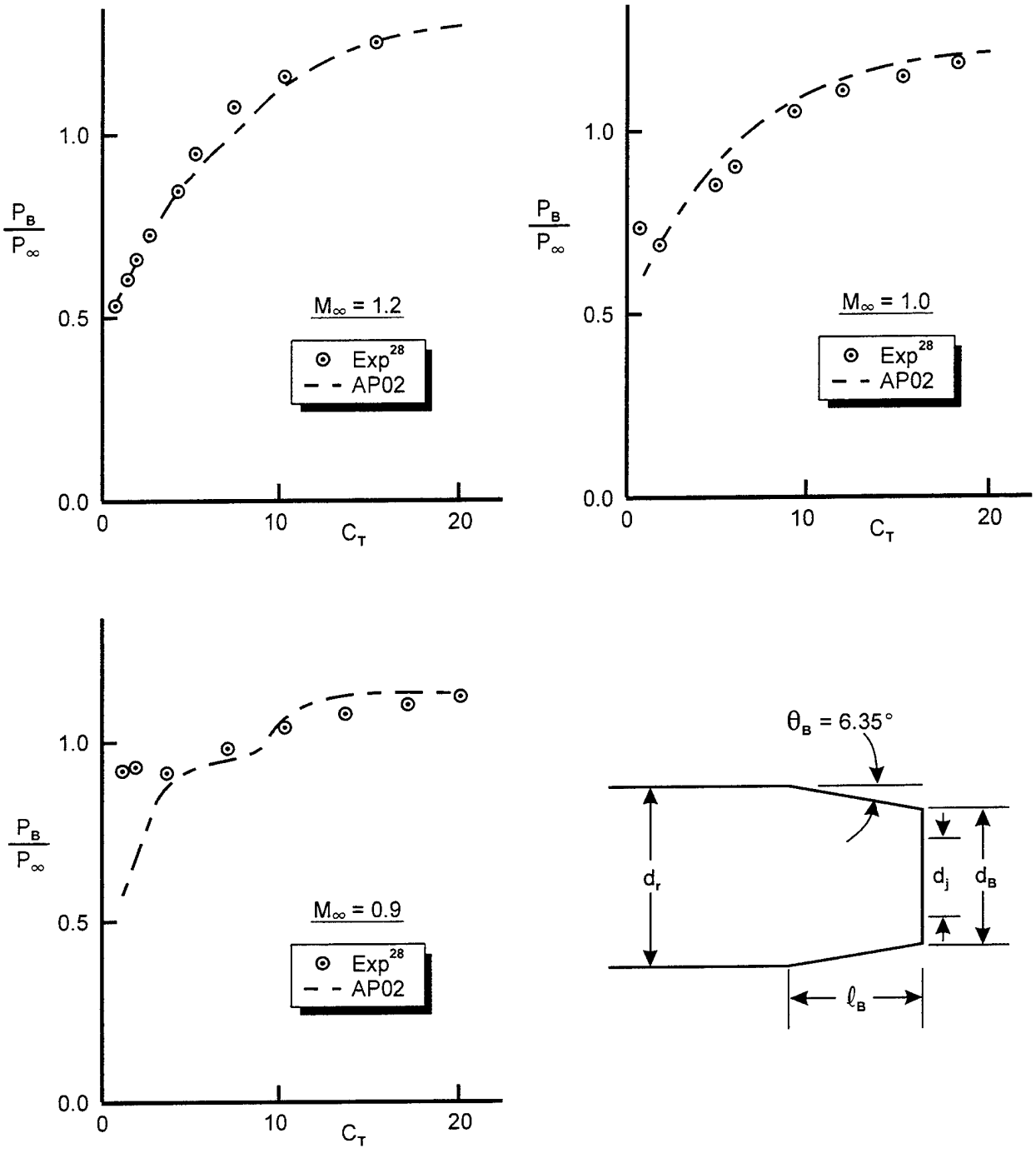

FIGURE 31. COMPARISON OF POWER-ON-BASE PRESSURE PREDICTION WITH EXPERIMENT FOR BOATTAIL AFTERBODY (dj/dr = 0.45; θj = 20 DEG; θ_B = 6.35 DEG; ℓ_B = 0.82 CAL; M_j = 2.7)

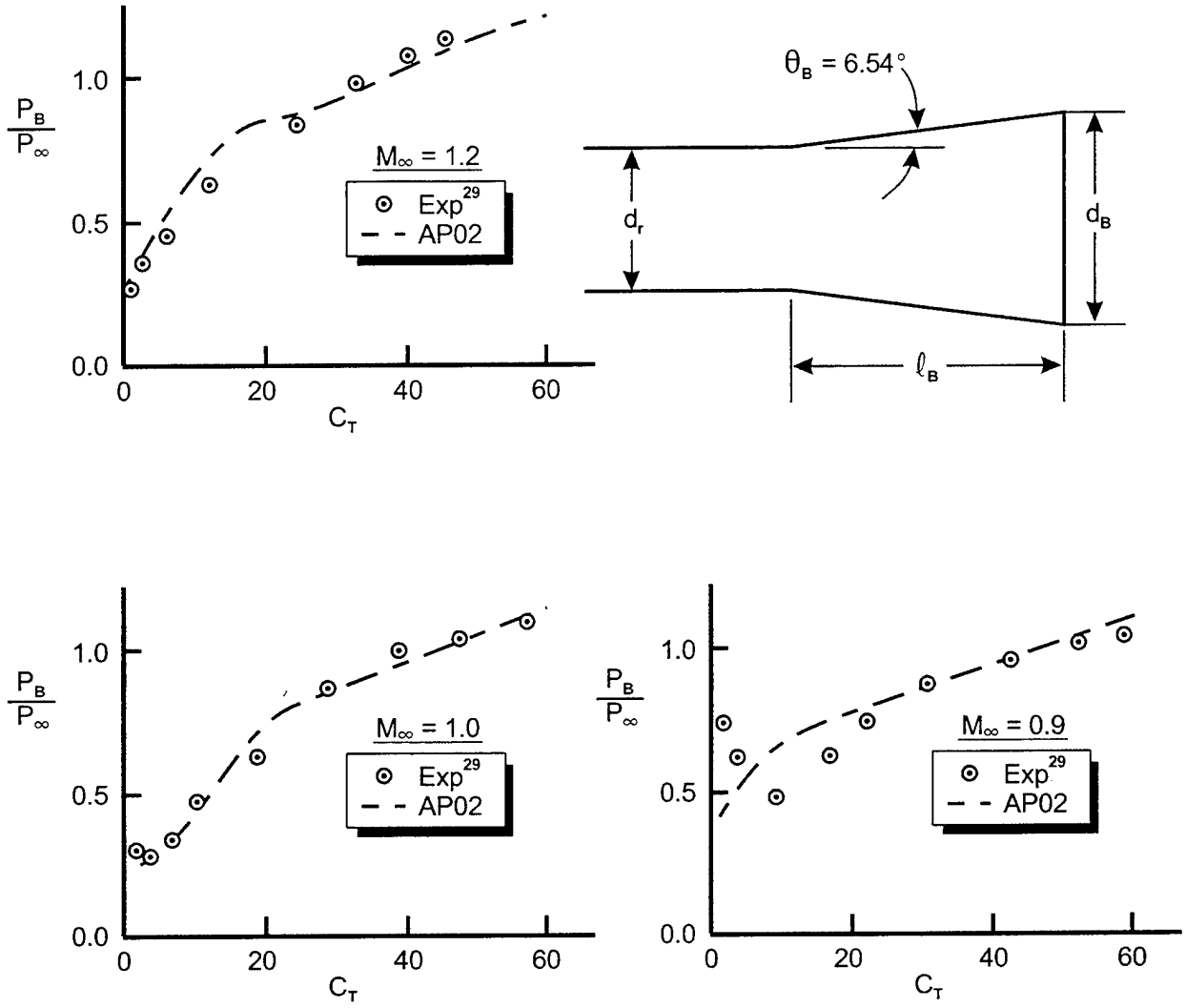

FIGURE 32. COMPARISON OF POWER-ON BASE PRESSURE PREDICTION WITH EXPERIMENT FOR FLARE AFTERBODY (Mj = 2.7; dj/dr = 0.8; θj = 20 DEG; θ_B = 6.54 DEG; ℓ_B = 1.34 CAL)

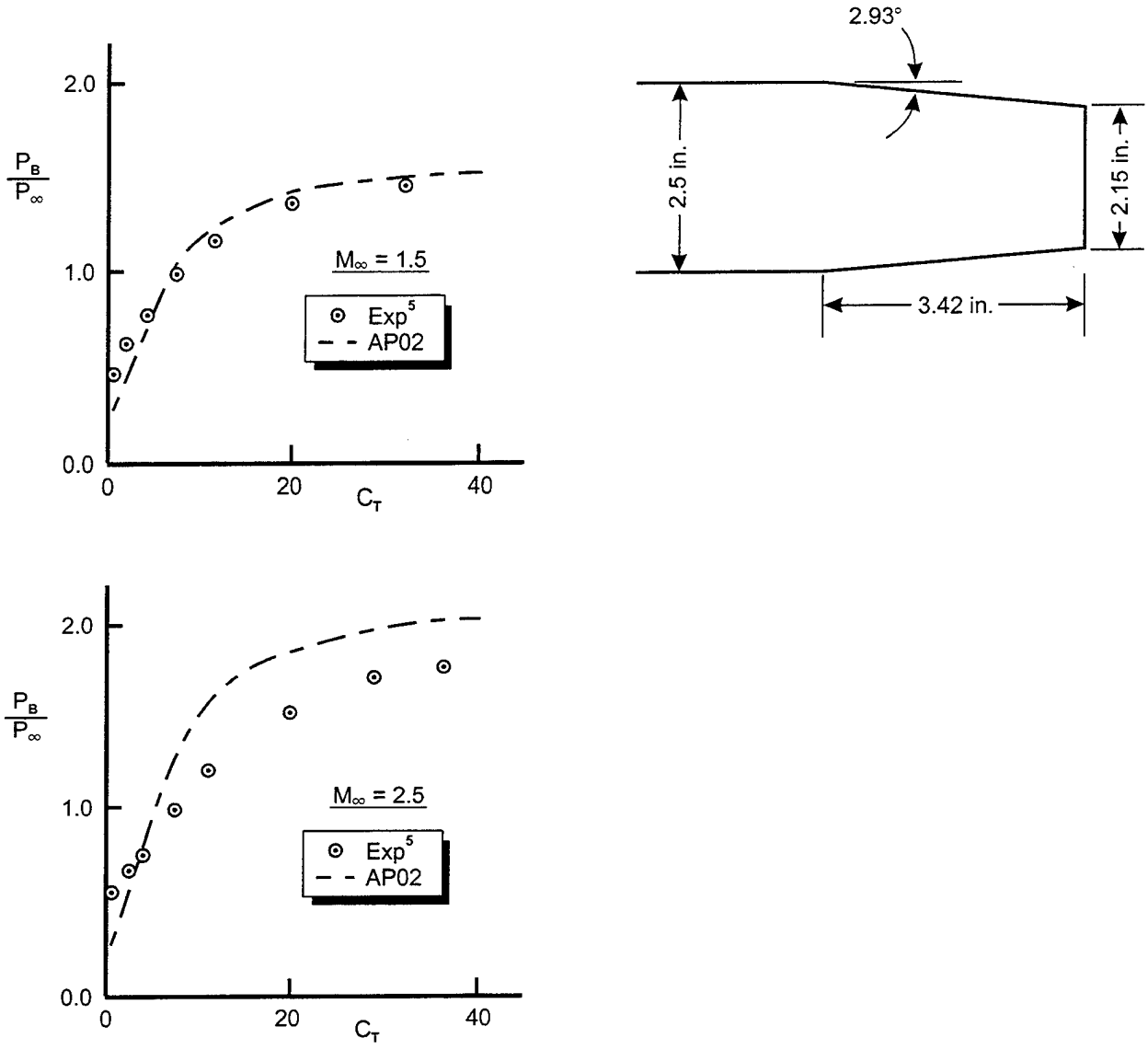

FIGURE 33. COMPARISON OF POWER-ON BASE PRESSURE PREDICTION WITH EXPERIMENT FOR A BOATTAILED AFTERBODY (Mj = 2.7; dj/dr = 0.45; θj = 20 DEG)

4.0 SUMMARY AND CONCLUSIONS

To summarize the comparison of experiment to the modified model of Danberg to predict base pressure at base bleed conditions, the following conclusions are drawn:

1. The modified theory gave good agreement to cold gas experimental data for all practical values of the injection parameter and ejector diameter ratio and at all Mach numbers where data was found. These values are typically $I \leq 0.005$ and $d_j/d_r \approx 0.4$. The theory was seen to be accurate for many conditions outside the practical range of applicability.

2. A relationship was derived for cold gas conditions where the maximum value of I as a function of the ejector diameter ratio could be used with accurate values of base pressure ratio expected. For hot gas conditions, this cold gas upper limit was reduced by about one third.

3. In general, the semiempirical theory applicability range increases with decreasing Mach numbers (larger values of I allowed).

4. For limited hot gas comparisons of theory and experiment, it was seen that the theory gave acceptable agreement to the data. It was also seen that the optimum value of I is much lower than for cold gas conditions.

5. While base bleed is an effective way to reduce drag and increase range, a properly designed boattail can achieve the same amount of drag reduction as base bleed from a fairly square-based projectile, but with better accuracy and lower cost.

To summarize the power-on base drag prediction method for rockets, an improved semiempirical method has been developed. It is patterned after the method of Brazzel and Henderson[1] but has been modified significantly to make it more robust in terms of values of thrust coefficient allowed, freestream Mach numbers allowed, and afterbody geometries allowed. In comparing the new method to experimental data, it was seen to give reasonable comparisons to most databases. However, it was found that not all experimental data were consistent, so part of the poor comparisons with some cases is believed to be experimental measurement problems. While the new method has been validated with various types of afterbodies (boattail, flare, or cylinder), it has not been validated at angle of attack or when fins were present. It is assumed that the change in base pressure due to the presence of fins and angle of attack at power-off conditions can be applied directly to the power–on base pressure predictions.

While the present improved semiempirical power-on base pressure prediction method is believed to be an improvement over existing empirical techniques, additional work is still needed in this area. For example, the present method does not account for nozzle exit angle. Additional

validations (and possible modifications of the method) are needed for angle of attack and fin effects as well.

5.0 REFERENCES

1. Brazzel, Charles E. and Henderson, J. H., "An Empirical Technique for Estimating Power-On Base Drag of Bodies-of-Revolution With a Single Jet Exhaust," Proceedings of a Specialists' Meeting Sponsored by the AGARD Fluid Dynamics Panel, held in Melhouse, France, 5-8 Sep 1966.

2. Johnson, L. H., Subj: Approximate Engine-On Base Pressure Computations for Aerodynamic Computer Codes, NSWCDD Internal Memorandum K21 No. 82-11, 1 Feb 1983.

3. Danberg, J. E., *Analysis of the Flight Performance of the 155 mm M864 Base Burn Projectile*, BRL-TR-3083, Apr 1990.

4. Moore, F. G.; Hymer, T. C.; and Wilcox, F. J., Jr; *Improved Empirical Model for Base Drag Prediction on Missle Configurations Based on New Wind Tunnel Data*, NSWCDD/TR-92/509, Oct 1992.

5. Craft, J. C. and Brazzel, C. E., *An Experimental Investigation of Base Pressures on a Body of Revolution at High Thrust Levels and Freestream Mach Numbers of 1.5 to 2.87*, U.S. Army Missile Command, Redstone Arsenal, AL, Report No. RD-TM-70-6, Jul 1970.

6. Henderson, J. H., *An Investigation for Modeling Jet Plume Effects on Missile Aerodynamics*, TR RD-CR-82-25, U.S. Army Missile Command, Redstone Arsenal, AL 35809, Jul 1982.

7. Deep, R. A.; Henderson, J. H.; and Brazzel, C. E.; *Thrust Effects on Missile Aerodynamics*, RD-TR-71-9, U.S. Army Missile Command, Huntsville, AL 35809, May 1971.

8. Moore, F. G.; McInville, R. M.; and Hymer, T. C., *The 1998 Version of the NSWC Aeroprediction Code: Part I-Summary of New Theoretical Methodology*, NSWCDD/TR-98/1, Apr 1998.

9. Reid, J. and Hastings, R. C.; *The Effect of a Central Jet on the Base Pressure of a Cylindrical Afterbody in a Supersonic Stream*, Royal Aircraft Establishment Report No. Aero 2621, Dec. 1959 (Farnborough, England).

REFERENCES (Continued)

10. Bowman, J. E. and Clayden, W. A., "Cylindrical Afterbodies in Supersonic Flow with Gas Injection," AIAA Journal, Vol. 5, No. 8, pp.1524-1525, Aug 1967.

11. Bowman, J. E. and Clayden, W. A., "Cylindrical Afterbodies at $M_\infty = 2$ with Hot Gas Ejection," AIAA Journal, Vol. 6, No. 12, pp. 2429-2431, Dec 1968.

12. Valentine, D. T. and Przirembel, C. E. G., "Turbulent Axisymmetric Near-Wake at Mach Four With Base Injection," AIAA Journal, Vol. 8, No. 12, pp. 2279-2280, Dec 1970.

13. Mathur, T. and Dutton, J. C., "Base Bleed Experiments with a Cylindrical Afterbody in Supersonic Flow," AIAA 95-0062, 33RD Aerospace Science Meeting, Reno, NV, 9-12 Jan 1995.

14. Sykes, D. M., "Cylindrical and Boattailed Afterbodies in Transonic Flow with Gas Ejection," AIAA Journal, Vol. 8, No. 3, pp. 588-589, Mar 1970.

15. Kayser L. D., "Effects of Base Bleed and Supersonic Nozzle Injection on Base Pressure," Memorandum Report No. 2456, USA Ballistic Research Laboratories, Aberdeen Proving Ground, MD, Mar 1975. (AD B 003442L)

16. Cortright, E. M. Jr. and Schroeder, A. H., *Preliminary Investigation of Effectiveness of Base Bleed in Reducing Drag of Blunt Based Bodies in Supersonic Stream*, NACA RM E51A26 (1951).

17. Murthy, S. N. B. and Osborn, J. R., "Base Flow Phenomena With and Without Injection: Experimental Results, Theories and Bibliography," AIAA progress in Astronautics and Aeronauticss, Vol.40, 1976; also Aerodynamics of Base Combustion (same issue).

18. Kayser, L. D.; Kuzan, J. D., Vazquez, D. N., *Ground Testing for Base-Burn Projectile Systems*, BRL-MR-3708, U.S.A. Ballistic Research Laboratory, Aberdeen Proving Ground, MD. Nov 1988.

19. Badrinarayaman, M. A., "An Experimental Investigation of Base Flows at Supersonic Speeds," Journal of the Royal Aeronautical Society, Vol. 65, pp. 475-482, 1961.

20. Butler, C.; Sears, E; and Pellas, S., *Aerodynamic Characteristics of 2, 3, and 4 Caliber Tangent-Ogive Cylinders with Nose Bluffness Ratios of 0.00, 0.25, 0.50, and 0.75 at Mach Numbers From 0.6 to 4.0*, AFATL-TR-77-8, Jan 1977.

21. Spahr, J. R. and Dickey, R. R., *Effect of Tail Surfaces on the Base Drag of a Body of Revolution at Mach Numbers of 1.5 and 2.0*, NACA TN-2360, 1951.

REFERENCES (Continued)

22. Hill, F. K. and Alpher, R. A., *Base Pressure at Supersonic Velocities*, Johns Hopkins University, Bumblebee Report-106, Nov 1949.

23. Ding, Z.; Liu, Y.; and Chen, S., "A Study of Drag Reduction by Base Bleed at Subsonic Speeds," First International Symposium on Special Topics in Chemical Propulsion: Base Bleed, Athens, Greece, 23-25 Nov 1988.

24. Sahu, J., *Supersonic Flow Over Cylindrical Afterbodies with Base Bleed*, BRL Technical Report TR-2742, Aberdeen, MD, Jun 1986.

25. Schilling, H., "Experimental Investigation on the Base-Bleed-Effect for Body-Tail-Combinations," Proceedings of the 8th International Symposium on Ballistics, Amsterdam, Holland, 1984.

26. Bromm, A. F. and O'Donnell, R. M., *Investigation at Supersonic Speeds of the Effect of Jet Mach and Divergence Angle of the Nozzle Upon the Pressure of the Base Annulus of a Body of Revolution*, NACA RM E57E06, Aug 1957.

27. Martin, T. A. and Brazzel, C. E., *Investigation of the Effect of Low Thrust Levels on the Base Pressure of a Cylindrical Body at Supersonic Speeds*, USAMC, Redstone Arsenal, USA, RD-TR-70-11, May 1970.

28. Petrie, H. L. and Walker, B. J., "Comparison of Experiment and Computation for a Missile Base Region Flowfield With a Centered Propulsive Jet," AIAA 85-1618, AIAA 18th Fluid Dynamics and Plasmadynamics and Lasers Conference, Cincinnati, Ohio, 16-18 Jul 1985.

29. Rubin, D. V.; *A Transonic Investigation of Jet Plume Effects on Base and Afterbody Pressures of Boattail and Flare Bodies of Revolution*, U.S. Army Missile Command Report RD-TR-70-10, Redstone Arsenal, AL, Oct 1970.

6.0 SYMBOLS AND DEFINITIONS

A_{ref}	Reference area which is cross-sectional area of body (ft^2)
A_t	Area of rocket motor nozzle throat cross-section
c	Fin root chord (ft)
C_A	Axial force coefficient
C_{A_B} , C_{A_f} , C_{A_W}	Base, skin-friction and wave components of axial force coefficient, respectively
C_{P_B}	Base Pressure Coefficient
C_T	Thrust Coefficient
d	Diameter
F_1, F_2, F_3	Symbols defining parameters used in semiempirical model for base drag prediction
I	Nondimensional base bleed injection parameter
$\dot{m}$	Mass rate of flow (ρAV)
M	Mach number
P	Static pressure (lb/ft^2)
P_0	Total pressure (lb/ft^2)
RMF	Jet momentum flux ratio
t	Fin thickness at root chord (ft)
t_{tip}	Fin thickness at tip (ft)
t/c	Fin thickness-to-chord ratio

t/d	Fin thickness-to-body reference diameter ratio
T	Temperature (°R) or thrust (lbs)
V	Velocity (ft/sec)
x	Distance from body base to fin trailing edge (for $\delta = 0$ deg)
x_j	Distance of jet exit from body base (positive behind base)
x/c	Distance from body base to fin trailing edge (for $\delta = 0$ deg) in tail root chord lengths
α	Body angle of attack (deg) (positive nose up)
δ	Fin control deflection (positive leading edge up)
γ	Ratio of specific heats
ρ	Density (slugs/ft^3)

General Subscripts

B	Conditions at body base
C	Conditions in rocket motor chamber
j	Conditions at nozzle exit
r	Reference conditions
∞	Freestream conditions

Subscripts on C_{P_B}

f	C_{P_B} of body with flare
NF	C_{P_B} of body alone with no fins
t/c	C_{P_B} of body with fins of a given thickness-to-chord ratio
x/c	C_{P_B} of body with fins located a given distance from the body base in fin root chord lengths

α	C_{P_B} of body at a given angle of attack
δ	C_{P_B} of body with fins at a given deflection angle

Superscript

*	Indicates conditions where M = 1.0

DISTRIBUTION

DOD ACTIVITIES (CONUS)

	Copies
ATTN CODE 35 (ZIMET)	1
CODE 351 (MORRISON)	1
CODE 351 (GRAFF)	1
CODE 332FD (LEKOUDIS)	1
CHIEF OF NAVAL RESEARCH	
BALLSTON CENTRE TOWER ONE	
800 NORTH QUINCY ST	
ARLINGTON VA 22217-5660	
ATTN CODE 474T6OD (LOFTUS)	1
CODE 4732HOD (SMITH)	1
CODE 473COOD (PORTER)	1
CODE 47HOOOD (BOSS)	1
CODE 473COOD (MCMANIGAL)	1
CODE 47311OD (HOUSH)	1
CODE 47311OD (GLEASON)	1
CODE 4722EOD (JETER)	1
TECHNICAL LIBRARY	1
COMMANDER	
NAVAL AIR WARFARE CENTER	
WEAPONS DIVISION	
1 ADMINISTRATION CIRCLE	
CHINA LAKE CA 93555-6001	
ATTN TECHNICAL LIBRARY	1
G RUDACILLE PMS 38012 7	1
COMMANDER	
NAVAL SEA SYSTEMS COMMAND	
2531 JEFFERSON DAVIS HWY	
ARLINGTON VA 22242-5160	
ATTN TECHNICAL LIBRARY	1
COMMANDER	
NAVAL AIR SYSTEMS COMMAND	
47122 LILJENCRANTZ ROAD UNIT 7	
PATUXENT RIVER MD 20670-5440	

	Copies
ATTN C KLEIN	1
TECHNICAL LIBRARY	1
COMMANDER	
NAVAL AIR WARFARE CENTER	
WEAPONS DIVISION	
521 9TH ST	
POINT MUGU CA 93042-5001	
ATTN T C TAI	1
M J MALIA	1
TECHNICAL LIBRARY	1
COMMANDER	
NSWC	
CARDEROCK DIVISION	
WASHINGTON DC 20034	
ATTN R M HOWARD	1
TECHNICAL LIBRARY	1
SUPERINTENDENT	
NAVAL POSTGRADUATE SCHOOL	
1 UNIVERSITY CIRCLE	
MONTEREY CA 93943-5001	
ATTN HEAD WEAPONS DEPT	1
HEAD SCIENCE DEPT	1
SUPERINTENDENT	
UNITED STATES NAVAL ACADEMY	
121 BLAKE RD	
ANNAPOLIS MD 21402-5000	
ATTN DIAG DT 4T (PAUL MURAD)	2
DIRECTOR	
DEFENSE INTELLIGENCE AGENCY	
WASHINGTON DC 20301	
ATTN BRENT WAGGONER	1
CODE 4072 BLDG 2540	
NAVAL WEAPONS SUPPORT CENTER	
CRANE IN 47522-5000	

DISTRIBUTION (Continued)

	Copies
ATTN W T RITTER	1
DEPT OF AIR FORCE	
846TH TEST SQUADRON TGTM	
1521 TEST TRACK RD	
HOFFMAN AFB NM 88330-7847	
ATTN CODE 5252P (KRAUSE)	1
TECHNICAL LIBRARY	1
COMMANDER	
INDIAN HEAD DIVISION	
NAVAL SURFACE WARFARE CENTER	
101 STRAUSS AVE	
INDIAN HEAD MD 20640-5035	
ATTN TECHNICAL LIBRARY	1
COMMANDING GENERAL	
MARINE CORPS COMBAT	
DEVELOPMENT COMMAND	
2048 SOUTH ST	
QUANTICO VA 22134-5129	
ATTN E SEARS	1
L E LIJEWSKI	1
C COTTRELL	1
TECHNICAL LIBRARY	1
AFATL (ADLRA) (DLGC)	1
EGLIN AFB FL 32542-5000	
ATTN TECHNICAL LIBRARY	1
USAF ACADEMY	
COLORADO SPRINGS CO 80912	
ATTN B BLAKE (BLD 146)	1
J JENKINS (BLD 146)	1
TECHNICAL LIBRARY	1
COMMANDING OFFICER	
AFSC	
2210 8TH STREET	
WRIGHT PATTERSON AFB OH 45433	
ATTN JIM SIMON	1
NAIC TANW	
HQ NAIC TANW	
4115 HEBBLE CREEK ROAD SUITE 28	
WPAFB OH 45433-5623	

	Copies
ATTN J USSELTON	1
W B BAKER JR	1
TECHNICAL LIBRARY	1
ARNOLD ENGINEERING DEVELOPMENT	
CENTER USAF	
TULLAHOMA TN 37389	
ATTN H HUDGINS	1
G FRIEDMAN	1
AMSTA-AR-WEL-TL	1
COMMANDER	
US ARMY TACOM-ARDEC	
BUILDING 59 PHIPPS ROAD	
PICATINNY ARSENAL NJ 07806-5000	
ATTN R PUHALLA JR	1
W STUREK	1
C NIETUBICZ	1
A MIKHAIL	1
P PLOSTINS	1
TECHNICAL LIBRARY	1
COMMANDING GENERAL	
BALLISTIC RESEARCH LABORATORY	
ABERDEEN PROVING GROUND	
ABERDEEN MD 21005-5066	
ATTN DIRECTOR	1
INTERCEPTOR TECHNOLOGY	
BALLISTIC MISSILE DEFENSE OFFICE	
THE PENTAGON	
WASHINGTON DC 20350	
ATTN SFAE SD ASP	1
SFAE SD HED	1
DEPUTY COMMANDER	
US ARMY STRATEGIC DEFENSE COMMAND	
P O BOX 1500	
HUNTSVILLE AL 35807-3801	
ATTN D WASHINGTON	1
W WALKER	1
R KRETZSCHMAR	1
D FERGUSON JR	1
COMMAND GENERAL	
US ARMY MISSILE COMMAND	
AMSMI RD SS AT	
REDSTONE ARSENAL AL 35898-5252	

DISTRIBUTION (Continued)

	Copies
DEFENSE TECHNICAL INFORMATION CENTER 8725 JOHN J KINGMAN ROAD SUITE 0944 FORT BELVOIR VA 22060-6218	2
DIRECTOR DEFENSE PRINTING SERVICE BLDG 176 WASHINGTON NAVY YARD 901 M ST E WASHINGTON DC 20374-5087	1
ATTN CODE A76 TECHNICAL LIBRARY COMMANDING OFFICER CSSDD NSWC 6703 W HIGHWAY 98 PANAMA CITY FL 32407-7001	1
ATTN DR P WEINACHT AERODYNAMICS BRANCH PROPULSION AND FLIGHT DIV WTD AMSRL WT PB US ARMY RESEARCH LAB ABERDEEN PROVING GROUND MD 21005-5066	1
ATTN GREGG ABATE US AIR FORCE WRIGHT LABORATORY WL MNAA 101 W EGLIN BLVD STE 219 EGLIN AFB FL 32542-5000	1
ATTN JOHN GRAU US ARMY ARDEC COMMANDER US ARMY ARDEC AMSTA AR AET A BLDG 3342 PICATINNY ARSENAL NJ 07806-5000	1
ATTN FRANK MACDONALD NAWC CHINA LAKE COMMANDER CODE 473 20D NAVAIRWARCENNSDNDIV CHINA LAKE CA 93555	1
ATTN MARK LAMBERT NAWC CODE 4732HOD CHINA LAKE CA 93555	1
ATTN MICHAEL MUSACHIO DIRECTOR OFFICE OF NAVAL INTELLIGENCE 4251 SUITLAND ROAD (ONI 2321) WASHINGTON DC 20395	1
ATTN DR ALAN NICHOLSON MSC 5B DEFENSE INTELLIGENCE AGENCY MISSILE AND SPACE INTELLIGENCE CTR REDSTONE ARSENAL AL 35898-5500	1
ATTN EDWARD HERBERT US ARMY MISSILE COMMAND AMSMI RD MG GA BLDG 5400 ROOM 250 REDSTONE ARSENAL AL 35898	1
ATTN PAUL KOLODZIEJ NASA AMES RESEARCH CENTER MS 234 1 MOFFETT FIELD CA 94035	1
ATTN LCDR T HARTLINE USNR R NR ONI 2109 NAVAL RESERVE UNIT 112 CRESTVIEW CIRCLE MADISON AL 35758	1
ATTN CODE 4732HOD DAVID HALL PROPULSION PERFORMANCE OFFICE NAVAL AIR WARFARE CTR WEAPONS DIV 1 ADMINISTRATIVE CIR CHINA LAKE CA 93555-6001	1
ATTN DONALD SHEREDA WL FIMA BLDG 450 2645 FIFTH ST STE 30 WRIGHT PATTERSON AFB OH 45433-7936	1
BMDO AQS 1725 JEFFERSON DAVIS HWY STE 809 ARLINGTON VA 22202	1
ATTN JEFFREY RANDORF US ARMY SPACE AND STRATEGIC DEFENSE COMMAND P O BOX 1500 CSSD-BC-SS 106 WYNN DRIVE HUNTSVILLE AL 35807-3801	1

DISTRIBUTION (Continued)

NON-DOD ACTIVITIES (CONUS)

	Copies
NICHOLS RESEARCH CORPORATION MS 912 P O BOX 400002 4040 S MEMORIAL PKWY HUNTSVILLE AL 35815-1502	1
THE CNA CORPORATION P O BOX 16268 ALEXANDRIA VA 22302-0268	1
GIDEP OPERATIONS OFFICE CORONA CA 91720	1
ATTN TECHNICAL LIBRARY NASA AMES RESEARCH CENTER MOFFETT CA 94035-1099	1
ATTN C SCOTT D CURRY NASA JOHNSON SPACE CENTER HOUSTON TX 77058	1 1
ATTN TECHNICAL LIBRARY NASA WASHINGTON DC 20546	1
ATTN B HENDERSON D MILLER J ALLEN F WILCOX TECHNICAL LIBRARY NASA LANGLEY RESEARCH CENTER HAMPTON VA 23365	1 1 1 1 2
ATTN DR K JONES NASA MARSHALL SPACE FLIGHT CTR CODE TD63 MSFC AL 35812	1
ATTN D G MILLER (L 219) TECHNICAL LIBRARY LAWRENCE LIVERMORE NATIONAL LABORATORY EARTH SCIENCES DIVISION UNIVERSITY OF CALIFORNIA P O BOX 808 LIVERMORE CA 94551	1 1
ATTN DR F MOORE AEROPREDICTION INC 12341 MILLBANK RD KING GEORGE VA 22485	3
ATTN W RUTLEDGE (1635) R LAFARGE R EISLER TECHNICAL LIBRARY SANDIA NATIONAL LABORATORY P O BOX 5800 ALBUQUERQUE NM 87185-5800	1 1 1 1
ATTN WALT GUTIERREZ SANDIA NATIONAL LABORATORIES MAIL STOP 0825 P O BOX 5800 ALBUQUERQUE NM 87185-0825	1
ATTN ASSISTANT DEFENSE COOPERATION ATTACHE EMBASSY OF SPAIN WASHINGTON DC 20016	1
DE/AVT DEFENSE EQUIPMENT STAFF BRITISH EMBASSY 3100 MASSACHUSETTS AVE NW WASHINGTON DC 20008-3688	1
ATTN ASO LO IS ISRAEL AIR FORCE LIAISON OFFICER 700 ROBBINS AVE PHILADELPHIA PA 19111	1
ATTN GERMAN MILITARY REP US OA GMR TRAFFIC AND TRANSPORTATION DIVISION 10 SERVICES ROAD DULLES INTERNATIONAL AP WASHINGTON DC 20041	1
ATTN PROF F R DEJARNETTE NORTH CAROLINA STATE UNIVERSITY DEPT OF MECHANICAL AND AEROSPACE ENGINEERING BOX 7921 RALEIGH NC 27695	1

DISTRIBUTION (Continued)

	Copies
ATTN PROF J A SCHETZ VIRGINIA POLYTECHNIC AND STATE UNIVERSITY DEPT OF AEROSPACE ENGINEERING BLACKSBURG VA 24060	1
ATTN J M WU C BALASUBRAMAYAN TECHNICAL LIBRARY THE UNIVERSITY OF TENNESSEE SPACE INSTITUTE TULLAHOMA TN 37388	1 1 1
ATTN R NELSON TECHNICAL LIBRARY UNIVERSITY OF NOTRE DAME DEPT OF AEROSPACE AND MECHANICAL ENGINEERING BOX 537 NOTRE DAME IN 46556	1 1
ATTN PROF F NELSON DEPT OF MECH AND AERO ENG UNIVERSITY OF MISSOURI ROLLA ROLLA MO 65401	1
ATTN ROBERT ENGLAR GEORGIA TECH RESEARCH INSTITUTE AEROSPACE SCIENCE AND TECHNOLOGY LAB ATLANTA GA 30332	1
ATTN E LUCERO D FROSTBUTTER L PERINI TECHNICAL LIBRARY APPLIED PHYSICS LABORATORY JOHNS HOPKINS UNIVERSITY JOHNS HOPKINS ROAD LAUREL MD 20723-6099	1 1 1 1
ATTN B BROOKS R STANCIL R ELKINS LORAL VOUGHT SYSTEMS P O BOX 650003 M S EM 55 DALLAS TX 75265-0003	1 1 1
ATTN PROF J D ANDERSON DEPT OF AEROSPACE ENGINEERING UNIVERSITY OF MARYLAND COLLEGE PARK MD 20742	1
ATTN TECHNICAL LIBRARY HUGHES MISSILE SYSTEMS COMPANY P O BOX 11337 BLDG 802 MS A1 OLD NOGALES HWY TUCSON AZ 83734-1337	1
ATTN M DILLENIUS NIELSEN ENGINEERING AND RESEARCH INC 526 CLYDE AVE MOUNTAIN VIEW CA 95043	1
ATTN J XERIKOS N CAMPBELL TECHNICAL LIBRARY MCDONNEL DOUGLAS ASTRONAUTICS CO (WEST) 5301 BOLSA AVE HUNTINGTON BEACH CA 92647	1 1 1
ATTN J WILLIAMS S VUKELICH J FIVEL R GERBSCH (CODE 1111041) TECHNICAL LIBRARY MCDONNELL DOUGLAS ASTRONAUTICS CO (EAST) BOX 516 ST LOUIS MO 63166-0516	1 1 1 1 1
ATTN TECHNICAL LIBRARY UNITED TECHNOLOGIES NORDEN SYSTEMS NORWALK CT 06856	1
ATTN T LUNDY D ANDREWS TECHNICAL LIBRARY LOCKHEED MISSILES AND SPACE CO INC P O BOX 1103 HUNTSVILLE AL 35807	1 1 1

DISTRIBUTION (Continued)

	Copies
ATTN W CHRISTENSON	1
D WARNER	1
ALLIANT TECHSYSTEMS INC	
600 SECOND ST NE	
HOPKINS MN 55343	
ATTN TECHNICAL LIBRARY	1
B SALEMI	1
J BOUDREAU	1
RAYTHEON COMPANY	
MISSILE SYSTEMS DIVISION	
P O BOX 1201	
TEWKSBURY MA 01876-0901	
ATTN JOSEPH ANDRZEJEWSKI	1
MEVATEC CORP	
1525 PERIMETER PARKWAY	
SUITE 500	
HUNTSVILLE AL 35806	
ATTN DR G S SCHMIDT	1
LORAL DEFENSE SYSTEMS	
1210 MASSILLON ROAD	
AKRON OH 44315-0001	
ATTN W NORDGREN 721	1
GOULD INC OSD	
18901 EUCLID AVE	
CLEVELAND OH 44117	
ATTN TECH LIBRARY	1
AEROJET ELECTRONIC SYSTEMS	
P O BOX 296 III	
AZUSA CA 91702	
ATTN P READING	1
G CHRUSCIEL	1
TECHNICAL LIBRARY	1
LOCKHEED MISSILES AND SPACE CO INC	
P O BOX 3504	
SUNNYVALE CA 94088	
ATTN K C LEE	1
AEROTHERM CORP	
580 CLYDE AVE	
MOUNTAIN VIEW CA 94043	

	Copies
ATTN TECH LIBRARY	1
FMC NAVAL SYSTEMS DIV	
4800 E RIVER ROAD	
MINNEAPOLIS MN 55421-1402	
ATTN JAMES SORENSON	1
VINCENT ALLEN	1
ORBITAL SCIENCES	
3380 SOUTH PRICE ROAD	
CHANDLER AZ 85248	
ATTN RON EFROMSON	1
MIT LINCOLN LABORATORY	
244 WOOD STREET	
LEXINGTON MA 02173-0073	
ATTN BRIAN WALKUP	1
ALLEGHENY BALLISTICS LAB	
210 STATE ROUTE 956 WV01-13	
ROCKET CENTER WV 26726-3548	
ATTN DR T LIN	1
TRW ELECTRONICS AND DEFENSE SECTOR	
BLDG 527/RM 706	
P O BOX 1310	
SAN BERNADINO CA 92402	
ATTN G VINCENT	1
SPARTA INC	
4901 CORPORATE DR	
HUNTSVILLE AL 35805	
ATTN M S MILLER	1
N R WALKER	1
DYNETICS INC	
P O DRAWER B	
HUNTSVILLE AL 35814-5050	
ATTN H A MCELROY	1
GENERAL DEFENSE CORP	
P O BOX 127	
RED LION PA 17356	
ATTN ENGINEERING LIBRARY	1
ARMAMENT SYSTEMS DEPT	
GENERAL ELECTRIC CO	
BURLINGTON VT 05401	

DISTRIBUTION (Continued)

	Copies
ATTN TECHNICAL LIBRARY OAYNE AERONAUTICAL 2701 HARBOR DRIVE SAN DIEGO CA 92138	1
ATTN BRIAN EST BOEING ST LOUIS P O BOX 516 ST LOUIS MO 63166-0516	1
ATTN WILLIAM FACINELLI ALLIED SIGNAL P O BOX 22200 MS 1207 3B TEMPE AZ 85285	1
ATTN DR T P SHIVANANDA TRW BMD P O BOX 1310 SAN BERNADINO CA 92402-1313	1
ATTN T R PEPITONE AEROSPACE TECHNOLOGY INC P O BOX 1809 DAHLGREN VA 22448	1
ATTN ERIC MOORE MAIL STOP MER 24 1281 LOCKHEED SANDERS P O BOX 868 NASHUA NH 03061	1
ATTN DR BRIAN LANDRUM RI BLDG E33 PROPULSION RESEARCH CENTER UNIVERSITY OF ALABAMA HUNTSVILLE AL 35899	1
ATTN JIM ROBERTSON RESEARCH SOUTH INC 555 SPARKMAN DRIVE SUITE 818 HUNTSVILLE AL 35816-3423	1
ATTN BOB WHYTE ARROW TECH ASSOCIATES INC 1233 SHELBURNE ROAD D8 SO BURLINGTON VT 05403	1
ATTN JUAN AMENABAR SAIC 4001 NORTH FAIRFAX DRIVE STE 800 ARLINGTON VA 22209	1
ATTN TECHNICAL LIBRARY TELEDYNE RYAN AERONAUTICAL 2701 HARBOR DRIVE SAN DIEGO CA 92138	1
ATTN DR KIRIT PATEL SVERDRUP TECHNOLOGY INC TEAS GROUP BLDG 260 P O BOX 1935 EGLIN AFB FL 32542	1
ATTN FRANK LANGHAM MICRO CRAFT TECHNOLOGY 740 4TH ST MS 6001 ARNOLD AFB TN 37389	1
ATTN LAURA AYERS DELTA RESEARCH INC 315 WYNN DRIVE SUITE 1 HUNTSVILLE AL 35805	1
ATTN BRIAN BENNETT MCDONNELL DOUGLAS MC 064 2905 P O BOX 516 ST LOUIS MO 63166-0516	1
ATTN THOMAS FARISS LOCKHEED SANDERS P O BOX 868 MER24 1206 NASHUA NH 03061-0868	1
ATTN COREY FROST LOCKHEED MISSILES & SPACE CO INC P O BOX 070017 6767 OLD MADISON PIKE SUITE 220 HUNTSVILLE AL 35807	1

DISTRIBUTION (Continued)

	Copies
ATTN JEFFREY HUTH KAMAN SCIENCES CORPORATION 2560 HUNTINGTON AVE ALEXANDRIA VA 22303	1
ATTN WILLIAM JOLLY KAMAN SCIENCES 600 BLVD SOUTH SUITE 208 HUNTSVILLE AL 35802	1
ATTN STEPHEN MALLETTE KBM ENTERPRISES 15980 CHANEY THOMPSON RD HUNTSVILLE AL 35803	1
ATTN DONALD MOORE NICHOLS RESEARCH CORPORATION 4040 SOUTH MEMORIAL PARKWAY P O BOX 400002 MS 920C HUNTSVILLE AL 35815-1502	1
ATTN NANCY SWINFORD LOCKHEED MISSILES & SPACE CO P O BOX 3504 ORG E5-40 BLDG 1575E SUNNYVALE CA 94088-3504	1
ATTN DAVID RESSLER TRW BALLISTIC MISSILES DIV MS 953 2420 P O BOX 1310 SAN BERNARDINO CA 92402	1
ATTN MARK SWENSON ALLIANT TECHSYSTEMS MN11 262B 600 SECOND STREET NE HOPKINS MN 55343	1
ATTN LEROY M HAIR COLEMAN RESEARCH CORP 6820 MOQUIN DRIVE HUNTSVILLE AL 35806	1
ATTN SCOTT ALLEN ALLEN AERO RESEARCH 431 E SUNNY HILLS RD FULLERTON CA 92635	1
ATTN DARRYL HALL SAIC 1100 FIRST AVENUE SUITE 300 KING OF PRUSSIA PA 19406	1
ATTN SAMUEL HICKS III TEXAS INSTRUMENTS 6600 CHASE OAKS BLVD MS 8490 PLANO TX 75086	1
ATTN BARRY LINDBLOM ALLIANT DEFENSE ELECTRONICS SYSTEMS INC P O BOX 4648 CLEARWATER FL 34618	1
ATTN DR SHIN CHEN THE AEROSPACE CORP M4 967 P O BOX 92957 LOS ANGELES CA 90009	1
ATTN EUGENE HART SYSTEM PLANNING CORP 1000 WILSON BLVD ARLINGTON VA 22209	1
ATTN ELAINE POLHEMUS ROCKWELL AUTONETICS & MISSILE SYSTEMS DIVISION D611 DL23 1800 SATELLITE BLVD DULUTH GA 30136	1
ATTN MICHAEL GLENN TASC 1992 LEWIS TURNER BLVD FT WALTON BEACH FL 32547	1
ATTN STEVEN MARTIN SYSTEMS ENGINEERING GROUP INC 9841 BROKEN LAND PARKWAY SUITE 214 COLUMBIA MD 21046-1120	1

DISTRIBUTION (Continued)

	Copies
ATTN C W GIBKE LOCKHEED MARTIN VOUGHT SYSTEMS MS SP 72 P O BOX 650003 DALLAS TX 75265-0003	1
ATTN CHRIS HUGHES EDO GOVERNMENT SYSTEMS DIV 1500 NEW HORIZONS BLVD AMITYVILLE NY 11701-1130	1
ATTN DANIEL LESIEUTRE NIELSEN ENGINEERING & RES INC 526 CLYDE AVENUE MOUNTAIN VIEW CA 94043-2212	1
ATTN THOMAS LOPEZ COLEMAN RESEARCH CORP 990 EXPLORER BLVD HUNTSVILLE AL 35806	1
ATTN JENNIE FOX LOCKHEED MARTIN VOUGHT SYSTEMS P O BOX 650003 MS EM 55 DALLAS TX 75265-0003	1
ATTN JOHN BURKHALTER AUBURN UNIVERSITY 211 AEROSPACE ENGR BLDG AUBURN UNIVERSITY AL 36849	1
ATTN DR MAX PLATZER NAVAL POSTGRADUATE SCHOOL DEPT OF AERONAUTICS & ASTRONAUTICS CODE AA PL MONTEREY CA 93943	1
ATTN MIKE DANGELO MIT LINCOLN LABORATORY 1745 JEFFERSON DAVIS HWY 1100 ARLINGTON VA 22202	1
ATTN RICHARD HAMMER JOHNS HOPKINS APPLIED PHYSICS LAB JOHNS HOPKINS ROAD LAUREL MD 20723-6099	1
ATTN MAURICE TUCKER BATTELLE HUNTSVILLE OPERATIONS 7501 S MEMORIAL PKWY STE 101 HUNTSVILLE AL 35802	1
ATTN STEVE MULLINS SIMULATION AND ENGINEERING CO INC 4935 CENTURY ST NW HUNTSVILLE AL 35816-1901	1
ATTN ROBERT BRAENDLEIU KAISER MARQUARDT 16555 SATICOY ST VAN NUYS CA 91406-1739	1
ATTN LAWRENCE FINK BOEING AIRCRAFT AND MISSILES P O BOX 3707 MC 4A 36 SEATTLE WA 98124-2207	1
ATTN ROY KLINE KLINE ENGINEERING CO INC 27 FREDON GREENDELL RD NEWTON NJ 07860-5213	1
ATTN THOMAS KLAUSE TRW P O BOX 80810 ALBUQUERQUE NM 87198	1
ATTN DAN PLATUS THE AEROSPACE CORPORATION P O BOX 92957 LOS ANGELES CA 90009	1
ATTN DR REX CHAMBERLAIN TETRA RESEARCH CORPORATION 2610 SPICEWOOD TR HUNTSVILLE AL 35811-2604	1
ATTN PERRY PETERSEN NORTHROP GRUMMAN CORP DEPT 9B51 MAIL ZONE XA 8900 EAST WASHINGTON BLVD PICO RIVERA CA 90660-3783	1

DISTRIBUTION (Continued)

	Copies
ATTN DR JAMES HAUSER AERO SPECTRA INC 2850 KENYON CIRCLE P O BOX 3006 BOULDER CO 80307	1
ATTN DARRELL AUSHERMAN TRW SPACE AND DEFENSE ONE SPACE PARK MAIL STATION R1-1062 REDONDO BEACH CA 90278-1071	1
ATTN JAY EBERSOHL ADVATECH PACIFIC INC 2015 PARK AVENUE SUITE 8 REDLANDS CA 92373	1
ATTN LAYNE COOK UNIVERSAL SPACE LINES 8620 WOLFF CT SUITE 110 WESTMINSTER CO 80030	1
ATTN PAUL WILDE ACTA INC 2790 SKYPARK DR SUITE 310 TORRANCE CA 90505-5345	1
ATTN DR MICHAEL HOLDEN CALSPAN UB RESEARCH CENTER P O BOX 400 BUFFALO NY 14225	1
ATTN RICHARD GRABOW SPACE VECTOR CORP 17330 BROOKHURST ST SUITE 150 FOUNTAIN VALLEY CA 92708	1
ATTN BRENT APPLEBY DRAPER LABORATORY 555 TECHNOLOGY SQ MS77 CAMBRIDGE MA 02139	1
ATTN JAMES JONES SPARTA INC 1901 N FORT MYER DR SUITE 600 ARLINGTON VA 22209	1
ATTN SCOTT HOUSER PHOENIX INTEGRATION 1872 PRATT DRIVE SUITE 1835 BLACKSBURG VA 24060	1
ATTN S ROM MURTY TELEDYNE BROWN ENGINEERING MS 200 300 SPARKMAN DRIVE HUNTSVILLE AL 35807	1
ATTN STUART COULTER SVERDRUP TECHNOLOGY 670 2ND ST MS4001 ARNOLD AIR FORCE BASE TULLAHOMA TN 37389-4001	1
ATTN DR RICHARD HOWARD NAVAL POSTGRADUATE SCHOOL DEPT OF AERONAUTICS AND ASTRONAUTICS CODE AA HO NPS MONTEREY CA 93943	1
ATTN J BRENT RUMINE MIT LINCOLN LABORATORY 244 WOOD STREET BUILDING S ROOM 52-327 LEXINGTON MA 02173-9185	1
NON-DOD ACTIVITIES (EX-CONUS)	
ATTN A BOOTH BRITISH AEROSPACE DEFENCE LTD MILITARY AIRCRAFT DIVISION WARTON AERODROME WARTON PRESTON LANCASHIRE PR4 1AX UNITED KINGDOM	1
ATTN R CAYZAC GIAT INDUSTRIES 7 ROUTE DE GUERCY 18023 BOURGES CEDEX FRANCE	1
ATTN MAJ F DE COCK ECOLE ROYALE MILITAIRE 30 AV DE LA RENAISSANCE 1040 BRUXELLES BELGIUM	1

DISTRIBUTION (Continued)

	Copies
ATTN J EKEROOT BOFORS MISSILES 691 80 KARLSKOGA SWEDEN	1
ATTN CH FRANSSON NATIONAL DEFENCE RESEARCH ESTABLISHMENT DEPT OF WEAPON SYSTEMS EFFECTS AND PROTECTION KARLAVAGEN 106B 172 90 SUNDBYBERG SWEDEN	1
ATTN M HARPER BOURNE DEFENCE RESEARCH AGENCY Q134 BUILDING RAE FARNBOROUGH HAMPSHIRE QU14 6TD UNITED KINGDOM	1
ATTN A H HASSELROT FFA P O BOX 11021 161 11 BROMMA SWEDEN	1
ATTN B JONSSON DEFENCE MATERIAL ADMINISTRATION MISSILE TECHNOLOGY DIVISION 115 88 STOCKHOLM SWEDEN	1
ATTN P LEZEAUD DASSAULT AVIATION 78 QUAI MARCEL DASSAULT 92214 SAINT CLOUD FRANCE	1
ATTN J LINDHOUT N L R ANTHONY FOKKERWEG 2 1059 CM AMSTERDAM THE NETHERLANDS	1
ATTN A MICKELLIDES GEC MARCONI DEFENCE SYSTEMS LTD THE GROVE WARREN LANE STANMORE MIDDLESEX UNITED KINGDOM	1
ATTN K MOELLER BODENSEEWERK GERAETETECHNIK GMBH POSTFACH 10 11 55 88641 UBERLINGEN GERMANY	1
ATTN RIBADEAU DUMAS MATRA DEFENSE 37 AV LOUIS BREGUET BP 1 78146 VELIZY VILLACOUBLAY CEDEX FRANCE	1
ATTN R ROGERS DEFENCE RESEARCH AGENCY BLDG 37 TUNNEL SITE CLAPHAM BEDS MK 41 6AE UNITED KINGDOM	1
ATTN S SMITH DEFENCE RESEARCH AGENCY Q134 BUILDING RAE FARNBOROUGH HAMPSHIRE QU14 6TD UNITED KINGDOM	1
ATTN J SOWA SAAB MISSILES AB 581 88 LINKOPING SWEDEN	1
ATTN D SPARROW HUNTING ENGINEERING LTD REDDINGS WOOD AMPTHILL BEDFORDSHIRE MK452HD UNITED KINGDOM	1

DISTRIBUTION (Continued)

	Copies
ATTN P STUDER DEFENCE TECHNOLOGY AND PROCUREMENT AGENCY SYSTEMS ANALYSIS AND INFORMATION SYSTEMS DIVISION PAPIERMUEHLESTRASSE 25 3003 BERNE SWITZERLAND	1
ATTN J M CHARBONNIER VON KARMAN INSTITUTE 72 CHAUSSEE DE WATERLOO 1640 RHODE SAINT GENESE BELGIUM	1
ATTN P CHAMPIGNY DIRECTION DE L AERONAUTIQUE ONERA 29 AV DE LA DIVISION LECLERC 92320 CHATILLON SOUS BAGNEUX CEDEX FRANCE	1
ATTN DR P HENNIG DEUTSCHE AEROSPACE (DASA) VAS 414 ABWEHR AND SCHUTZ POSTFACH 801149 8000 MUENCHEN 80 GERMANY	1
ATTN DR S J YOON AGENCY FOR DEFENSE DEVELOPMENT AERODYNAMICS DIVISION (4-3-1) P O BOX 35-4 YUSEONG TAEJON KOREA	1
ATTN PETER CAAP HD FLIGHT SYS DEPT FAA AERONAUTICAL RESEARCH INST OF SWEDEN BOX 11021 BROMMA SWEDEN 16111	1
ATTN DAVE BROWN WEAPON SYSTEMS DIVISION AERONAUTICAL AND MARITIME RESEARCH LABORATORY P O BOX 1500 SALISBURY SOUTH AUSTRALIA 5108	1

INTERNAL		Copies
B		1
B04		1
B04	(ZIEN)	1
B05	(STATON)	1
B10		1
B10	(HSIEH)	1
B51	(ARMISTEAD)	1
B60	(TECHNICAL LIBRARY)	3
C		1
CD222	(BECHTEL)	1
D		1
G		1
G02		1
G20		1
G205		1
G21		1
G21	(COOK)	1
G22		1
G23		1
G23	(BIBEL)	1
G23	(HANGER)	1
G23	(HARDY)	1
G23	(HYMER)	5
G23	(OHLMEYER)	1
G23	(ROWLES)	1
G23	(WEISEL)	1
G24		1
G24	(ROBINSON)	1
G30		1
G305		1
G32	(DAY)	1
G33	(FRAYSSE)	1
G33	(RINALDI)	1
G50		1
G50	(SOLOMON)	1
G60		1
G70		1
G72		1
G72	(CHEPREN)	1
K		1
K40		1
N		1
T		1
T13	(ALEXOPOULOS)	1
T406		1